

PERVAPORATION OF ORGANIC/WATER MIXTURES BY MFI TYPE  
ZEOLITE MEMBRANES SYNTHESIZED IN A FLOW SYSTEM

A THESIS SUBMITTED TO  
THE GRADUATE SCHOOL OF NATURAL AND APPLIED SCIENCES  
OF  
MIDDLE EAST TECHNICAL UNIVERSITY

BY

ÖZLEM DEDE

IN PARTIAL FULFILLMENT OF THE REQUIREMENTS  
FOR  
THE DEGREE OF MASTER OF SCIENCE  
IN  
CHEMICAL ENGINEERING

AUGUST 2007

Approval of the thesis:

**“PERVAPORATION OF ORGANIC/WATER MIXTURES BY MFI TYPE  
ZEOLITE MEMBRANES SYNTHESIZED IN A FLOW SYSTEM”**

submitted by **ÖZLEM DEDE** in partial fulfillment of the requirements for the degree of **Master of Science in Chemical Engineering Department, Middle East Technical University** by,

Prof. Dr. Canan Özgen  
Dean, Graduate School of **Natural and Applied Sciences** \_\_\_\_\_

Prof. Dr. Nurcan Baç  
Head of Department, **Chemical Engineering** \_\_\_\_\_

Assist. Prof. Dr. Halil Kalıpçılar  
Supervisor, **Chemical Engineering Dept., METU** \_\_\_\_\_

Prof. Dr. Ali Çulfaz  
Supervisor, **Chemical Engineering Dept., METU** \_\_\_\_\_

**Examining Committee Members:**

Prof. Dr. Müjgan Çulfaz  
Chemical Engineering Dept., Gazi University \_\_\_\_\_

Assist. Prof. Dr. Halil Kalıpçılar  
Chemical Engineering Dept., METU \_\_\_\_\_

Prof. Dr. Ali Çulfaz  
Chemical Engineering Dept., METU \_\_\_\_\_

Prof. Dr. Levent Yılmaz  
Chemical Engineering Dept., METU \_\_\_\_\_

Assist. Prof. Dr. Yusuf Uludağ  
Chemical Engineering Dept., METU \_\_\_\_\_

**Date:** 15.08.2007

**I hereby declare that all information in this document has been obtained and presented in accordance with academic rules and ethical conduct. I also declare that, as required by these rules and conduct, I have fully cited and referenced all material and results that are not original to this work.**

Name, Last name: Özlem Dede

Signature

## **ABSTRACT**

### **PERVAPORATION OF ORGANIC/WATER MIXTURES BY MFI TYPE ZEOLITE MEMBRANES SYNTHESIZED IN A FLOW SYSTEM**

Dede, Özlem

M.S., Department of Chemical Engineering

Supervisor: Assist. Prof. Dr. Halil Kalıpçılar

Co-Supervisor: Prof. Dr. Ali Çulfaz

August 2007, 79 Pages

Zeolite membrane synthesis is conventionally carried out in batch systems. Recently, several attempts have been performed to synthesize zeolite membranes in flow systems which can allow preparation of membranes with large specific surface areas.

Membranes synthesized in the recirculating flow system had comparable  $N_2/SF_6$  and  $n-C_4H_{10}/i-C_4H_{10}$  ideal selectivities with the membranes prepared in the batch system, indicating that good quality membranes can be produced by this method. The objective of this study is to separate organic/water mixtures by pervaporation by using MFI type membranes synthesized in the flow system. Effect of number of synthesis steps and synthesis method on the separation factor and flux was investigated.

Membranes were synthesized from clear solutions with a molar composition of 80SiO<sub>2</sub>:16TPAOH:1536H<sub>2</sub>O at 95°C and atmospheric pressure. The synthesis solution was recirculated through the tubular alumina support with a flow rate of 6 ml/min for 72 h. The membranes were characterized by X-ray diffraction for phase identification and scanning electron microscopy for morphology determination. Single gas permeances of N<sub>2</sub>, H<sub>2</sub>, CH<sub>4</sub>, CO<sub>2</sub>, n-C<sub>4</sub>H<sub>10</sub> and i-C<sub>4</sub>H<sub>10</sub> were measured between 25 and 200°C. Mixtures of 5 wt% ethanol/water, 2-propanol/water and acetone/water were separated by pervaporation at different temperatures.

The single gas permeances decreased with increasing temperature for weakly adsorbed gases. For n-C<sub>4</sub>H<sub>10</sub> the permeance passed through a maximum and i-C<sub>4</sub>H<sub>10</sub> permeance was nearly constant. For a membrane synthesized by two consecutive synthesis steps, the ideal selectivity for n-C<sub>4</sub>H<sub>10</sub>/i-C<sub>4</sub>H<sub>10</sub> was 132 at 200°C. The selectivity in the pervaporation separation of ethanol-water mixture was 43 with a permeate flux of 0.2 kg/m<sup>2</sup>h at 25°C. With increasing temperature, selectivity decreased but the flux increased, the selectivity was 23 and the flux was 1.9 kg/m<sup>2</sup>h at 85°C. 2-propanol/water and acetone/water separation factors were 36 and 1024 with 0.2 and 0.1 kg/m<sup>2</sup>h fluxes, respectively. The separation factors and fluxes for membranes synthesized in the flow system were comparable with membranes synthesized in the batch system.

Keywords: Zeolite membranes, MFI, Flow system, Pervaporation

## ÖZ

### SÜREKLİ SİSTEMDE SENTEZLENMİŞ MFI TİPİ ZEOLİT MEMBRANLAR KULLANILARAK PERVAPORASYONLA ORGANİK/SU KARIŞIMLARININ AYRIŞTIRILMASI

Dede, Özlem

Yüksek Lisans, Kimya Mühendisliği Bölümü

Tez Danışmanı: Y.Doç.Dr. Halil Kalıpçılar

Ortak Tez Danışmanı: Prof. Dr. Ali Çulfaz

Ağustos 2007, 79 sayfa

Zeolit membranlar geleneksel olarak kesikli sistemlerde sentezlenir. Son yıllarda, daha yüksek yüzey alanına sahip geometrilerde membran üretilmesini sağlayabilecek olan akış sisteminde sentez üzerine çalışmalar yürütülmektedir.

Sürekli sistemde sentezlenmiş membranlar, kesikli sistemde sentezlenen membranlarla kıyaslanabilir  $N_2/SF_6$  ve  $n-C_4H_{10}/i-C_4H_{10}$  ideal seçicilikleri göstermiş ve bu yöntemle iyi kalitede membranlar üretileceği gösterilmiştir. Bu çalışmanın amacı, sürekli sistemde sentezlenmiş membranları kullanarak organik/su karışımlarını pervaporasyon ile ayırmaktır. Sentez metodunun ve ardışık sentezin ayırma seçiciliği ve akı üzerindeki etkisi araştırılmıştır.

Membranlar  $80SiO_2:16TPAOH:1536H_2O$  mol bileşiminde berrak çözeltiler kullanılarak  $95\text{ }^\circ\text{C}$ ' de ve atmosfer basıncında sentezlenmiştir. Sentez çözeltisi 6

ml/dak hızında 72 saat süreyle membran yüzeyinden geçirilmiştir. Sentezlenen membranlar X-ışınımı kırınımı ve elektron mikroskobu ile karakterize edilmiştir. N<sub>2</sub>, H<sub>2</sub>, CH<sub>4</sub>, CO<sub>2</sub>, n-C<sub>4</sub>H<sub>10</sub> ve i-C<sub>4</sub>H<sub>10</sub> gazlarının tek gaz geçirgenlikleri 25 ve 200°C arasında ölçülmüştür. %5 etanol/su, 2-propanol/su ve aseton/su karışımlarının pervaporasyon yöntemi ile değişik sıcaklıklarda ayrılması çalışılmıştır.

Adsorplanma enerjisi az olan gazlar için sıcaklık artışıyla birlikte tek gaz geçirgenliklerinin azaldığı gözlemlenmiştir. n-C<sub>4</sub>H<sub>10</sub> geçirgenliği sıcaklık artışıyla birlikte maksimumdan geçmiş, i-C<sub>4</sub>H<sub>10</sub> geçirgenliği ise sıcaklık değişiminden etkilenmemiştir. n-C<sub>4</sub>H<sub>10</sub>/i-C<sub>4</sub>H<sub>10</sub> ideal seçiciliği yüksek sıcaklıkta 132 olarak bulunmuştur. Aynı membran için etanol/su karışımı seçicilik değeri 43, akı da 0.2 kg/m<sup>2</sup>s'dir. Sıcaklıkla beraber seçicilik azalmış, akı artmıştır. 85°C'de ayırma seçiciliği 23 akı da 1.9 kg/m<sup>2</sup>s olarak ölçülmüştür. 2-propanol/su ve aseton/su seçicilikleri 36 ve 1024 olup, akılar da 0.2 kg/m<sup>2</sup>h ve 0.1 kg/m<sup>2</sup>s'dir. Sürekli sistemde sentezlenen membranlar, kesikli sistemde sentezlenen membranlarla kıyaslanabilir akı ve seçicilik değerleri göstermiştir.

Anahtar kelimeler: Zeolit membranlar, MFI, Sürekli sistem, Pervaporasyon

*To Necla and Hüseyin Dede*



## **ACKNOWLEDGEMENT**

I would like to express my gratitude to my supervisor Assist. Prof. Dr. Halil Kalıpçılar for his detailed and constructive comments, continuous encouragement, and motivation throughout this study. I am also deeply thankful to my co-supervisor Prof. Dr. Ali Çulfaz for his constructive criticism, guidance and support.

I would like to thank to Prof. Dr. Birgül Tantekin Ersolmaz and Dr. Çiğdem Oral Atalay in Istanbul Technical University for the Scanning Electron Micrographs.

I am thankful to the people in the Machine Shop for their help in constructing various components for the setup.

I would like to thank to Belma Soydaş for her friendship, encouragement, and helps in the laboratory. I am grateful to Volkan Değirmenci for his comments during the construction of the set-up and general support. I deeply thank to my friends; Değer Şen, Sezin Akbay, Canan Gücüyener, Engin Özkol and Onur Kaçar for their motivation and support.

Project grant of METU-BAP-2006-07-02-00-01 and TUBITAK-106M176 scholarship are gratefully acknowledged.

## TABLE OF CONTENTS

ABSTRACT.....	iv
ÖZ.....	vi
DEDICATION.....	viii
ACKNOWLEDGEMENTS.....	ix
TABLE OF CONTENTS.....	x
LIST OF TABLES.....	xiii
LIST OF FIGURES.....	xiv
CHAPTERS	
1. INTRODUCTION.....	1
2. LITERATURE SURVEY.....	4
2.1 Introduction to membranes.....	4
2.2. Zeolite membranes.....	5
2.3. Description of MFI type zeolites.....	7
2.4. Synthesis of zeolite membranes by hydrothermal synthesis.....	8
2.5. Synthesis in continuous systems.....	9
2.6. Pervaporation.....	10
2.7. Use of zeolite membranes in pervaporation separations.....	14
2.7.1. Use of MFI type zeolite membranes for pervaporation separations...	15
2.7.2. Factors affecting pervaporation performance of MFI membranes.....	18

3. EXPERIMENTAL METHODS.....	22
3.1. Membrane synthesis.....	22
3.1.1. Materials.....	22
3.1.2. Membrane seeding.....	22
3.1.3. Membrane synthesis in the recirculating flow system.....	24
3.1.4. Membrane synthesis in the batch system.....	26
3.2. Template removal and initial characterization.....	26
3.3 Membrane Characterization.....	27
3.3.1. Measuring single gas permeances.....	27
3.2.Pervaporation.....	30
4. RESULTS AND DISCUSSION.....	35
4.1. Characterization of membranes.....	35
4.2. Single gas permeances before calcination.....	40
4.3. Single gas permeances after calcination.....	40
4.3.1. Effect of temperature on single gas permeation.....	45
4.3.2. Comparison of n-C <sub>4</sub> H <sub>10</sub> /i-C <sub>4</sub> H <sub>10</sub> selectivities with literature.....	46
4.4. Pervaporation separation of organic/water mixtures.....	49
4.4.1. Effect of number of synthesis parameters on separation factor and flux.....	50
4.4.2. Variation of separation factor for different organics.....	51
4.4.3 Variation of separation factor and flux with time.....	52
4.4.4. Variation of separation factor and flux with temperature.....	53

4.4.5. Pure component pervaporation measurements for membrane F2.....	55
4.4.6. Comparison of pervaporation fluxes with literature.....	58
5. CONCLUSIONS.....	60
RECOMMENDATIONS.....	62
REFERENCES.....	63
APPENDICES	
A. CALIBRATION PLOTS FOR THE PERVAPORATION MEASUREMENTS..	68
B. RAW DATA FOR GAS PERMEATION EXPERIMENTS.....	71
C. RAW DATA FOR PERVAPORATION EXPERIMENTS.....	72
D. PHOTOGRAPHS OF THE PERVAPORATION SET-UP.....	77
E. REFERENCES FOR FIGURE 4.12.....	78

## LIST OF TABLES

Table 2.1. Si/Al ratios, pore diameters and examples of performed separations for LTA, MFI and FAU membranes.....	6
Table 2.2. Separation factors and fluxes for zeolite A membranes for dehydration of ethanol.....	15
Table 2.3. Separation factors and fluxes for the MFI membranes.....	17
Table 3.1. Operating conditions of the X-ray diffractometer.....	27
Table 3.2. Operating conditions for the gas chromatograph.....	33
Table 4.1. Synthesis method, number of synthesis steps and N <sub>2</sub> permeances before calcination for the MFI membranes.....	35
Table 4.2. Ideal gas selectivities.....	43
Table 4.3. Comparison of n-C <sub>4</sub> H <sub>10</sub> and i-C <sub>4</sub> H <sub>10</sub> permeation results with literature...	48
Table 4.4. Separation factors and fluxes (kg/m <sup>2</sup> .h) for pervaporation of 5 wt. % organic/95 wt.% water feed at room temperature.....	49
Table 4.5. Ideal selectivities and separation factors for alcohol/water mixtures for membrane F2 .....	55
Table B.1. Gas permeabilities (mol/m <sup>2</sup> .Pa.s x 10 <sup>7</sup> ) at 25 °C.....	71
Table B.2. Gas permeabilities (mol/m <sup>2</sup> .Pa.s x 10 <sup>7</sup> ) at 200 °C.....	71

## LIST OF FIGURES

Figure 2.1. Schematic of a membrane.....	4
Figure 2.2. SEM image of an MFI type zeolite membrane on an alumina support.....	6
Figure 2.3. Channel structure of an MFI crystal.....	8
Figure 2.4. Schematic of a simple pervaporation unit.....	11
Figure 3.1. Schematic drawing of the dip-coating set-up.....	23
Figure 3.2. Schematic of the recirculating flow system used for membrane synthesis.....	24
Figure 3.3. Schematic of the single gas permeation setup.....	29
Figure 3.4. Schematic drawing of the pervaporation set-up.....	31
Figure 4.1. XRD patterns of membrane surfaces for membranes F3 and B2.....	36
Figure 4.2. XRD patterns of the residual powders.....	37
Figure 4.3. Cross-section micrographs of membranes.....	38
Figure 4.4. Surface micrographs of membranes.....	39
Figure 4.5. Single gas permeances as a function of kinetic diameter.....	41
Figure 4.6. Single gas permeances as a function of temperature.....	47
Figure 4.7. Variation of separation factor and flux for membrane F2 for 5 wt% acetone/water solution at room temperature.....	52
Figure 4.8. Variation of fluxes for pervaporation of 5wt% EtOH/water mixtures....	54
Figure 4.9. Variation of for separation factors for pervaporation of 5wt% EtOH/water mixtures.....	54
Figure 4.10. Pure component pervaporation fluxes with respect to temperature for membrane F2.....	56
Figure 4.11. Pure water flux and water flux in presence of organics for membrane F2 .....	57

Figure 4.12. Comparison of separation factors and fluxes for ethanol/water mixture separations with literature.....	59
Figure A.1. Variation of ethanol peak area with ethanol concentration in ethanol/water mixture (wt%).....	68
Figure A.2. Variation of 2-Propanol peak area with 2-propanol concentration in propanol/water mixture (wt%).....	69
Figure A.3. Variation of acetone peak area with acetone concentration in acetone/water mixture (wt%).....	69
Figure A.4. Variation of water peak area with water concentration in organic/water mixture (wt%).....	70
Figure C.1. Variation of separation factor and flux for membrane F1 for 5 wt% ethanol/water solution.....	72
Figure C.2. Variation of separation factor and flux for membrane F2 for 5 wt% ethanol/water solution.....	73
Figure C.3. Variation of separation factor and flux for membrane F3 for 5 wt% ethanol/water solution.....	73
Figure C.4. Variation of separation factor and flux for membrane B1 for 5 wt% ethanol/water solution.....	74
Figure C.5. Variation of separation factor and flux for membrane B2 for 5 wt% ethanol/water solution.....	74
Figure C.6. Variation of separation factor and flux for membrane F2 for 5 wt% 2-propanol/water .....	75
Figure C.7. Variation of separation factor and flux for membrane F1 for 5 wt% 2-propanol/water solution at room temperature.....	75
Figure C.8. Variation of separation factor and flux for membrane F2 for 5 wt% 2-acetone/water solution at room temperature.....	76
Figure C.9. Variation of separation factor and flux for membrane F1 for 5 wt% 2-acetone/water solution at room temperature.....	76
Figure D.1. Photographs of the pervaporation set-up.....	77

# CHAPTER 1

## INTRODUCTION

Zeolites are crystalline aluminosilicates with a framework structure [1]. Their three dimensional network is constructed with  $TO_2$  tetrahedra linked through oxygen atoms, where T represents Al or Si. The framework structure of zeolites contains regular channels or interlinked voids in the micropore range. The pore sizes of zeolites are in the order of magnitude of molecular dimensions, varying typically between 0.4-1.2 nm depending on their types. The well defined uniform pore openings with molecular dimensions together with selective adsorption properties make zeolites suitable as membrane materials.

Zeolite membranes are thin films of zeolite crystals deposited on a porous and mechanically stable support. More than 14 zeolite structures have been prepared as membranes [2] and MFI is a widely studied structure due to its ease of preparation and suitable pore size for separation of mixtures of commercial importance.

A membrane should provide high permeability and selectivity at the same time to be used in industrial applications. Moreover a large surface area which can be manufactured with a high reproducibility is required together with cost-effective fabrication [4]. Up to now, the membrane quality is tried to be improved by modification of chemical gel composition [5-9] and variation of crystallization conditions [10, 11]. Zeolite membranes are typically prepared on discs or tubular supports with permeable areas around 5-15  $cm^2$ . Therefore scale up is required to increase the total surface area of the membrane to fulfill demands in industrial applications. Moreover, studies show that membranes with thicknesses typically



around 20  $\mu\text{m}$  are required to have defect-free samples [9]. The fluxes of membranes with that much thickness on the other hand are quite low to be commercialized. Therefore; thin layers of zeolite membranes with good quality is required to combine high permeability with high selectivity.

Zeolite membranes are conventionally synthesized by in situ hydrothermal synthesis in batch systems. In hydrothermal synthesis, a zeolite layer is grown onto a porous support in which the support material is immersed into an autoclave filled with synthesis gel or solution. Syntheses are usually carried out at high temperatures around 150-200  $^{\circ}\text{C}$ . Batch synthesis in gels has major drawbacks in terms of not providing uniform synthesis conditions throughout the support for producing membranes with high surface area/volume ratios. The non-uniform synthesis conditions may result in a non-uniform membrane thickness due to settling of crystals from the bulk and also unwanted phases might form.

As an alternative way to conventional synthesis several attempts have been performed to synthesize zeolite membranes in semi-continuous [15], continuous [16] and recirculating flow systems [17]. In a recirculating flow system much more homogeneous synthesis conditions can be provided around membrane and this can enable synthesis of membranes with high surface area/volume ratios. In the study of Çulfaz et al. [17], MFI type zeolite membranes were synthesized in a recirculating flow system where the synthesis solution is flown over the porous support. Due to the flow, the settling of crystals from bulk has less likely occurred, and as a result thin (1-2  $\mu\text{m}$ ) and uniform zeolite membranes were produced. These membranes had  $\text{N}_2/\text{SF}_6$  ideal selectivities between 9.1-14.9 at room temperature and  $n\text{-C}_4\text{H}_{10}/i\text{-C}_4\text{H}_{10}$  (50/50%) separation selectivities between 6.1–7.6 at 200 $^{\circ}\text{C}$ ; indicating that good quality thin membranes can be produced by this method.

The separation mechanism of zeolite membranes is by molecular sieving if the mixture to be separated has components with large differences in kinetic diameters.

Separation also takes place by preferential adsorption and differences in diffusion rates of molecules and this property of zeolite membranes enable separation of components with similar kinetic diameters. Also the contribution of flow through non-zeolite pores should not be neglected since it affects the separation factor and permeance. Zeolite membranes are used to for the separation of gas mixtures; separation of mixtures of hydrocarbons and light gases are widely studied. Zeolite membranes are also used for separation of liquid mixtures by pervaporation which is a membrane based separation technology. Organic/organic separations, organic/water separations and isomer separations are all accomplished by using zeolite membranes in pervaporation applications. Zeolite A type membranes were also commercialized for alcohol dehydration by pervaporation [22, 4]. The separation factors and fluxes for MFI membranes are not enough to be commercialized for pervaporation applications, significant research is going on to improve separation properties of these membranes for liquid mixtures.

Thin membranes with high separation factors and fluxes are desired for pervaporation applications. In this study, thin MFI membranes were synthesized on tubular alumina supports by the recirculating flow system. Pervaporation separation of ethanol/water, 2-propanol/water and acetone/water mixtures was performed. The performance of this novel synthesis method to separate liquid mixtures was investigated.

## CHAPTER 2

### LITERATURE SURVEY

#### 2.1 Introduction to membranes

A membrane is a selective barrier between two phases and selectively permeates components of a mixture with the aid of a driving force [18]. The components that selectively pass through the membrane are named as permeate and the remaining as retentate (Figure 2.1). The driving force across the membrane can be gradients of pressure, concentration or electrical potential [18].

Figure 2.1. Schematic of a membrane

Based on the structure, membranes can also be classified as dense, porous and composite membranes. Porous membranes can be either symmetric or asymmetric. Dense membranes are used for separation process of small molecules, however they

exhibit low fluxes. The thickness of symmetric polymeric membranes is between 10-200  $\mu\text{m}$ . Asymmetric membranes have dense top layers with a thickness around 0.1-0.5  $\mu\text{m}$ , and a porous sublayer with a thickness around 50-150  $\mu\text{m}$ . These membranes combine the high selectivity of a dense membrane with the high permeability of a thin membrane [18].

Another classification can be made based on material; organic and inorganic. Organic membranes are commonly used in industry but porous inorganic membranes show better temperature and chemical stabilities when compared to organic polymer membranes. Zeolite membranes are inorganic membranes that have a crystallographically determined monodispersed pore system which enables separation of gases or liquid mixtures due to the molecular sizes of the components [4].

## **2.2. Zeolite membranes**

A zeolite membrane consists of a thin, selective zeolite layer on top of a macroporous support. The thickness of the zeolite layer which functions as the membrane vary between 0.5-100  $\mu\text{m}$ . The macroporous support provides mechanical strength with small contribution to selectivity slightly hindering the flux [19]. Figure 2.2 shows a SEM image of an MFI type zeolite membrane on a macroporous alumina support.

Zeolites are built up of a three dimensional network of  $\text{SiO}_4$  and  $\text{AlO}_4$  tetrahedra and have uniform pore sizes. Over 130 framework types known today MFI, LTA and FAU structures are widely studied as membranes. Table 2.1 shows the Si/Al ratios, pore diameters and examples of performed separations for these membranes. LTA has a three dimensional structure and its pore size depend on the type of the cation in the framework.  $\text{Ca}^{2+}$ ,  $\text{Na}^+$ ,  $\text{K}^+$  makes the pore sizes 0.5 nm, 0.4 nm and 0.3 nm, respectively. MFI has a two dimensional structure and its pore diameters are between

0.51-0.56 nm. Silicalite and ZSM-5 are types of MFI membranes. FAU type zeolites, which include zeolites X and Y, have 0.75 nm pore dimensions.

Figure 2.2. SEM image of an MFI type zeolite membrane on an alumina support

Table 2.1. Si/Al ratios, pore diameters and examples of performed separations for LTA, MFI and FAU membranes

<b>Membrane Type</b>	<b>Si/Al ratio</b>	<b>Pore Diameter (nm)</b>	<b>Examples of performed separations</b>
<b>LTA</b>	1	0.40	H <sub>2</sub> O/EtOH, H <sub>2</sub> O/i-PrOH Mixtures of N <sub>2</sub> , O <sub>2</sub> , CH <sub>4</sub> , CO <sub>2</sub> , SF <sub>6</sub>
<b>MFI</b>	20-∞	0.55	EtOH/H <sub>2</sub> O, i-PrOH/H <sub>2</sub> O, MeOH/MTBE, Acetone/MEK, p-xylene/o-xylene; n-C <sub>4</sub> /i-C <sub>4</sub> , n-C <sub>6</sub> /o-xylene
<b>FAU</b>	1.3-2.5	0.75	H <sub>2</sub> O/EtOH, CO <sub>2</sub> /CH <sub>4</sub> , CO <sub>2</sub> /N <sub>2</sub> , C <sub>6</sub> /C <sub>8</sub>

The Si/Al ratios in the framework differ for different membrane types. It is reported in literature that increasing Al content makes the zeolite more hydrophilic [20-23]. The high Al content of the LTA and FAU membranes makes them suitable for dehydration applications. With increasing Si/Al ratio hydrophobicity, thermal stability and acid strength increases [4]. High thermal and chemical stability makes the high silica MFI membranes attractive for industrial applications [24]. The hydrophobic MFI membranes are used for removal of organic compounds and organic/organic separations.

### **2.3. Description of MFI type zeolites**

MFI (Mobile Five) structure has a three dimensional network consisting of sinusoidal channels (0.51 x 0.55 nm) which perpendicularly intersect straight channels (0.53 x 0.56 nm). Figure 2.3 shows the channel structure of an MFI crystal. There are 10 membered rings of Si and Al. MFI structure may be of two types: ZSM-5 or silicalite. The difference between these two is the aluminum content in the framework. ZSM-5 structure has a Si/Al ratio between 10-200 [25] whereas silicalite has no Al in the framework. Besides introducing hydrophilicity to the framework, Al presence provides catalytic activity and ion-exchange properties.

The pore diameters being close to commercially important molecules, high thermal and chemical stability makes MFI structure attractive for industrial applications [24]. Synthesis of MFI type zeolites have been widely studied, therefore a lot is known about its crystallization.

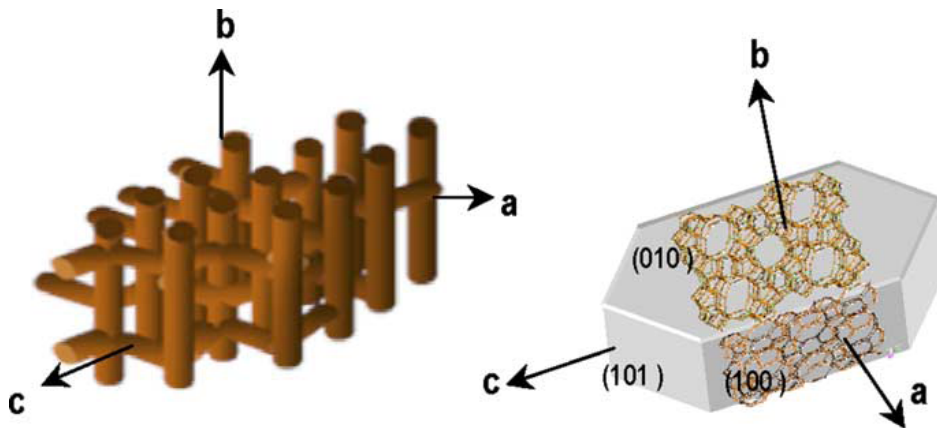


Figure 2.3. Channel structure of an MFI crystal. Direction b denotes the straight channels and a denotes sinusoidal channels [26]

#### 2.4. Synthesis of zeolite membranes by hydrothermal synthesis

Zeolite membranes are conventionally synthesized in autoclaves by hydrothermal synthesis. In hydrothermal synthesis a zeolite layer is crystallized onto a porous support by inserting the support material into the synthesis solution or gel. The synthesis solution together with the support is then placed in an autoclave and heated up to the synthesis temperature.

For MFI synthesis the synthesis solution is mainly composed of water, amorphous silica and a structure directing organic template. There are also some studies in literature to prepare membranes without organic template molecules [27, 67] to reduce the risk of crack formation during calcination. Membrane support is sometimes seeded prior to synthesis step to provide sites for zeolite growth and improve the control of crystal growth [2]. This technique is known as two-step crystallization and used to prepare oriented zeolite membranes [29, 30].

Support materials are usually alumina or stainless steel.  $\alpha$ -alumina and  $\gamma$ - alumina supports have pore diameters of 200 nm and 5 nm respectively. Pore diameters for

stainless steel supports vary between 500-4000 nm. Supports usually have tubular or disk geometries, membrane synthesis on monolith supports is also achieved [31].

MFI synthesis is usually carried out at high temperatures (150°C -200°C), there are also studies reporting synthesis at low temperatures such as 100°C [29, 57]. Synthesis at lower temperatures would be better for commercialization due to less energy consumption, but it is shown that the time required to reach 100 % yield is longer for synthesis at lower temperatures [58, 59].

The conventional synthesis method is difficult to scale up since it requires operation at high temperatures and cannot provide uniform synthesis conditions and it is not suitable for producing large area membranes. Synthesis in a continuous system can be better in terms of providing more uniform synthesis conditions.

## **2.5. Synthesis in continuous systems**

As alternatives to conventional hydrothermal synthesis, syntheses are also carried out with circulation or renewal of synthesis solution. Pina et al. [15] synthesized A type membranes on tubular supports in a semi-continuous system. In this system synthesis solution was withdrawn from the system and a fresh gel was supplied to the system from a reservoir. By this way, during a 5 hours synthesis period once in 13 minutes maximum, 75 minutes minimum; the synthesis solution was refreshed. Membranes were tested for 10%water/90%ethanol separation; selectivities were between 94-3603 with fluxes between 2.2-3.8 kg/m<sup>2</sup>.h.

Richter et al. [16] synthesized MFI type membranes on tubular supports and capillaries. The synthesis solution was continuously pumped from a reservoir to the membrane holder, and then discarded. Membranes synthesized in this study had thicknesses of 30 µm and membranes had H<sub>2</sub>/SF<sub>6</sub> selectivities between 22-31 with H<sub>2</sub> permeance around 4.0-4.7 x 10<sup>-7</sup> mol/m<sup>2</sup>.s.Pa.



Tsutsumi and Satoshi et al. [33] synthesized zeolite A layers on polytetrafluoroethylene substrates. In this study a circulation of synthesis solution was established and the solution was flown over the substrate. Synthesized layers were compared with layers synthesized in batch systems. Pure zeolite A layer was synthesized in the continuous system whereas for layers synthesized in batch systems some other zeolite phases were present.

Finally Çulfaz et al. [17] synthesized MFI membranes on tubular supports in a recirculating flow system. The synthesis solution was continuously recirculated over the support by using a peristaltic pump. Synthesis was carried out at 95 °C and atmospheric pressure. Uniform synthesis temperature was established by using a silicon oil bath. Thin (1-2 µm) and good quality membranes were synthesized by this method. Membranes had N<sub>2</sub>/SF<sub>6</sub> ideal selectivities between 9.1-14.9 at room temperature and n-C<sub>4</sub>H<sub>10</sub>/i-C<sub>4</sub>H<sub>10</sub> (50–50%) separation selectivities of 6.1–7.6 at 200°C.

Zeolite membrane synthesis is usually carried out by hydrothermal synthesis; use of flow systems is a new approach to membrane synthesis. Synthesis in flow systems can provide much more homogeneous synthesis conditions around the membrane and can enable synthesis of membranes with high surface area/volume ratios. With a few examples using different methods involving a flow system, Çulfaz et al. [17] had shown that good quality zeolite membranes can be produced by a recirculating flow system.

## **2.6. Pervaporation**

Pervaporation is a membrane based separation process to separate liquid mixtures. Figure 2.4 shows the schematic of a simple pervaporation unit. The feed side is kept at atmospheric pressure while the permeate side is kept under vacuum to provide the driving force for permeation. The vacuum is established by using a vacuum pump so

that the permeate pressure is kept lower than the saturation pressure of the compounds in the mixture at the separation temperature. The permeate stream, rich in the preferentially permeating component, is condensed in the condenser. The retentate stream which is rich in non-preferentially permeating component is either recycled back or used in another process.

Figure 2.4. Schematic of a simple pervaporation unit

Pervaporation involves the following steps:

- Selective sorption into the membrane on the feed side
- Selective diffusion through the membrane
- Desorption into a vapor phase on the permeate side [18]

Pervaporation allows separation of mixtures that are difficult to separate by more conventional techniques like distillation, extraction and sorption [2]. This process is mainly used to separate a minor amount of liquid from a liquid sample. Pervaporation is an attractive separation technology when the liquid mixture exhibits an azeotropic composition where distillation cannot be used. Pervaporation is also advantageous for separation of close-boiling mixtures.

Pervaporation is used to remove a small amount of a sample from a liquid sample; it may not be advantageous to use pervaporation for the complete separation. However, a combination of distillation and pervaporation can be applied to break the azeotrope, where the actual separation is performed by distillation and pervaporation is only applied to shift the composition from the azeotrope. The use of hybrid process, combination of pervaporation and distillation, is in many cases advantageous in terms of capital cost and operating cost [18].

Pervaporation is applied for:

- Dehydration applications (removal of water from organic solvents)
- Removal of volatile organic compound from water
  - Alcohols from fermentation broths
  - Volatile organic contaminants from waste water
  - Removal of flavour and aroma compounds
  - Removal of phenolics
- Polar/non-polar separations
  - Alcohols/Aromatics (methanol/toluene)
  - Alcohols/Aliphatics (ethanol/hexane)

- Alcohols/Ethers (methanol/methyl-t-butylether)
- Aromatics/Aliphatics (cyclohexane/benzene, hexane/toluene)
- Isomers (xylene isomers)

Polymeric membranes are widely used in pervaporation applications while research is in progress for the use of zeolite membranes. Zeolite membranes offer several advantages over polymeric membranes such as chemical and thermal stability. Zeolite membranes have molecular sized pores that cause differences in transport rates, and allow molecular sieving in some cases [2].

The separation performance of zeolite membranes are defined in terms of flux and selectivity.

Flux through a membrane is defined as:

Where  $W$  is the weight of permeate collected,  $A$  is the membrane permeable area and  $t$  is the operation time.

Separation factor is used to express the separation performance of binary mixtures. It is the ratio of the concentrations in the permeate stream divided by that in the feed for the two components. For separation of gas mixtures instead of feed compositions, the retentate compositions are used. Use of feed composition is common in liquid separations, because the retentate is usually recycled back to the feed tank.

Separation factor is defined as:

Where  $Y$  and  $X$  are permeate and feed weight fractions respectively.

A good quality membrane is expected to have a high selectivity in combination with high flux. Usually the selectivity is increased by increasing membrane thickness since a thicker membrane can be more effective to cover defects in zeolite films but the additional resistance to transport reduces the permeability. Defect free thin films are required for industrial applications.

### **2.7. Use of zeolite membranes in pervaporation separations**

The selectivity of a zeolite membrane is determined by its hydrophobicity or hydrophilicity in addition to its shape selectivity which depends on the zeolite type and alumina content in the framework [39]. LTA and MFI type zeolite membranes are widely studied for pervaporation applications. FAU type zeolite membranes are also used for pervaporation.

Zeolite A membranes are commercialized for dehydration of ethanol by a Japanese firm, Mitsui Engineering and Shipbuilding Co.Ltd. The pore size of zeolite A is smaller than sizes of organic molecules but larger than size of water molecules; therefore the separation is based on molecular sieving. The sieving mechanism combined with high hydrophilicity of zeolite A membrane results in very good selectivities yielding more than 99 % water in the permeate. In the commercial application, a feed stream containing water, ethanol, isopropyl alcohol and acetone with an initial water concentration of around 10 % was dehydrated so that the water concentration was less than 2 % in the permeate [4]. Table 2.2 shows the separation factors and fluxes for zeolite A membranes for ethanol dehydration. Membranes had shown selectivities around 4000 for ethanol dehydration. The reason of the high selectivity is the molecular sieving property of Zeolite A membrane for this separation.

FAU type membranes, like zeolite A membranes, are used for dehydration applications due to their hydrophilic structure. A flux of 1.6 kg/m<sup>2</sup>.h with a separation factor of 130 is reported for a FAU membrane for water/ethanol separation [4]. The separation by FAU type membranes is based on molecular interactions, not molecular sieving, due to the large pore structure [4].

Table 2.2. Separation factors and fluxes for zeolite A membranes for dehydration of ethanol

<b>Author</b>	<b>Support material</b>	<b>Temperature (°C)</b>	<b>% EtOH in feed</b>	<b>Separation Factor</b>	<b>Flux mol/m<sup>2</sup>h</b>	<b>Synthesis Method</b>
Kondo et al.[35]	Mullite/ alumina	50	95	4800	22	Batch
Holmes et al. [36]	Stainless steel	40	95	150	2.8	Batch
Okamoto et al.[37]	Alumina	35	90	1200	17	Batch
Pina et al. [15]	Alumina	125	90	3600	209	Semi continuous

In contrast to hydrophilic zeolite membranes, hydrophobic zeolite membranes remove organics from aqueous mixtures. Hydrophobic MFI membranes are used for organic/water and organic/organic separations.

### **2.7.1. Use of MFI type zeolite membranes for pervaporation separations**

Separation by MFI membranes is based on preferential adsorption of certain molecules rather than molecular sieving. In the case of organic/water separations, both organic and water molecules have sizes smaller than pore size of MFI. Although diffusion would seem to favor water permeation since water molecules have smaller sizes, hydrophobic effects dominate by preferentially adsorbing the organic compounds [39]. Therefore the permeate side of the MFI membrane is enriched by organic molecules. Table 2.3 shows the separation factors (S.F.) and fluxes for the MFI membranes in pervaporation separations.

The most common studied separation by MFI membranes is ethanol/water separation. Ethanol removal from fermentation broths is essential for production of biofuel. After fermentation is complete, ethanol purification is required. Purification separates ethanol from the other components of fermentation; of these components, water has the largest composition. This step is necessary because fuel purposes require very pure ethanol to properly blend with gasoline [47]. Lin et al. [40] reported the best membrane for this separation with a flux of  $0.9 \text{ kg/m}^2\cdot\text{h}$  and a separation factor of 106. The membranes were prepared by in situ crystallization and they concluded that in situ crystallization yielded better membranes when compared with seeding followed by crystallization. In this study membranes were also prepared on alumina supports and lower separation factors were observed. It was concluded that the silicalite membranes with higher Si/Al ratio showed better separation factors and fluxes.

Liu et al. [41] synthesized silicalite membranes on alumina supports by hydrothermal treatment. They have obtained low separation factors and fluxes for ethanol/water separation. The separation factor for methanol/water was improved from 3 to 15 when membrane was synthesized on a stainless steel support.

There are also studies to improve the hydrophobicity of the MFI membranes to increase the separation factor. Matsuda et al. [42] synthesized a silicone-coated silicalite membrane. The silicone was added to fill the non-zeolite pores. A high separation factor of 125 was obtained with a 0.14 kg/m<sup>2</sup>.h flux for the coated membrane. On the other hand the separation factor was 51 for the non-coated membrane synthesized under the same conditions. Silicone coating reduced the flux only with a fraction of 1 %. Bowen et al. [43] introduced germanium to the framework to increase the hydrophobicity. Germanium substituted membrane showed higher separation factors than the pure silicalite membrane.

Table 2.3. Separation factors and fluxes for the MFI membranes (at 30°C unless stated)

<b>Author</b>	<b>Membrane/ (Thickness)</b>	<b>Support</b>	<b>Feed</b>	<b>S.F.</b>	<b>Flux (mol/m<sup>2</sup>.h)</b>
Lin et al. [40]*	Silicalite (20-30 μm)	Mullite	(5%)EtOH /H <sub>2</sub> O	106	14 (0.9 kg/m <sup>2</sup> .h)
Liu et al. [41]	Silicalite (NA)	Alumina	(9.7%)EtOH /H <sub>2</sub> O	12	3.7 (0.1 kg/m <sup>2</sup> .h)
Matsuda et al. [42]	Silicalite (NA)	Stainless Steel	(4%) EtOH /H <sub>2</sub> O	125	3.7 (0.14 kg/m <sup>2</sup> .h)
Bowen et al. [43]	Ge-ZSM-5 (30 μm)	Stainless Steel	(5%) EtOH /H <sub>2</sub> O	47	6.9
Sano et al. [44]	Silicalite (400 μm)	Stainless Steel	(52%)MeOH /MTBE	9	3.5
Flanders et al. [45]	ZSM-5 (NA)	Stainless Steel	(50%)n-hexane/ 2,2-DMB	10	4.3
Yuan et al. [46]*	Silicalite (3-5 μm)	Alumina	(50%)p-xylene/ o-xylene	40	1.3

\*:60°C operation temperature



MFI membranes are also used for organic/organic separations. Flanders et al. [45] synthesized a ZSM-5 membrane on stainless steel support and observed a separation factor of 10 for n-hexane/ 2,2-DMB separation with a flux of 4.3 kg/m<sup>2</sup>h. Sano et al. [44] synthesized a silicalite membrane and the separation factor for MeOH/MTBE mixture was 9. The flux was quite high (3.5 mol/m<sup>2</sup>h) although the membrane was thick.

Zeolite membranes are used to separate vapor mixtures of xylene isomers, however there are also some pervaporation separation examples. Yuan et al. [46] synthesized membranes by a template free synthesis method. The separation factor and flux observed was 40 and 1.3 mol/m<sup>2</sup>h respectively.

The selectivities and fluxes of MFI membranes are not enough to be commercialized. Molecular simulation studies show that better selectivities can be obtained for MFI membranes [50]. Simulation results suggested that for ethanol/water mixture, ethanol might completely inhibit water permeance leading to an infinite separation factor for ethanol over water. There is a significant research to improve the separation performance of MFI membranes. It is concluded in literature that the design of more efficient membranes for removal of organic compounds must rely on improved selective adsorption characteristics of MFI zeolites [39].

### **2.7.2. Factors affecting pervaporation performance of MFI membranes**

Effect of **feed temperature** on pervaporation flux and selectivity is widely studied in literature. Increase in flux is observed with increasing temperature [31, 42, 48-51]. Transport through zeolite pores takes place by two mechanisms: adsorption and diffusion. For pervaporation applications, increase in temperature increases diffusion and therefore the flux. Since coverages still remain high at high temperatures,

diffusion effect dominates. Diffusion increases more than adsorption decreases [2] and fluxes increase with increasing temperature.

With increasing temperature, the selectivities may tend to increase [49, 31] or decrease [42, 50]. Decrease in selectivity for an organic/water mixture with temperature is due to increasing diffusion of water molecules together with a decrease in organic coverage. The increase in selectivity with temperature is due to increase in organic diffusion rate compensating the decrease in adsorption coverage.

Another factor affecting the separation factor for pervaporation is the **feed concentration**. For pervaporation of organic/water mixtures, an increase in organic concentration increases both the organic flux and total flux [41, 48, 51] since organics preferentially permeate through MFI pores. The separation factor on the other hand usually decreases with increasing organic concentration. The separation factor is a ratio of two ratios; the increase in the ratio in the denominator compensates the increase in numerator, yielding to a decrease in separation factor. The increase feed concentration compensates the increase in permeate concentration resulting in lower separation factors.

The driving force in pervaporation is the pressure difference across the membrane. An increase in **permeate pressure** would decrease the permeate flux. The pervaporation pressures at the permeate side are usually around 0.3-0.4 kPa or lower in literature.

The **feed pressure** has no effect on pervaporation fluxes since pressure has no significant effect on adsorption and permeation of liquid mixtures. In a molecular simulation study to understand pervaporation principles [39], the feed pressure was increased up to 1000 atm and only small changes were found in the separation factor. This shows that pervaporation is not a hydrostatically driven process; it is driven by

molecular forces. The pervaporation fluxes are independent of feed pressure and the pressure needs to be only enough to maintain a liquid feed.

Another factor affecting the separation factor and flux is **concentration polarization**. Concentration polarization is the feed concentration gradient caused by depletion of the preferentially permeating component at the membrane feed interface [2]. Studies were performed to understand the effect of concentration polarization on pervaporation performance. Tuan et al. [49] reported selectivities and fluxes for pervaporation designs both as dead end and cross-flow. In a dead-end design, the feed mixture is stationary and hydrostatically flows to the membrane surface. In the cross flow design the feed mixture is circulated so that the feed mixture facing the membrane surface is mixed to reduce concentration polarization. MeOH/water, EtOH/water and PrOH/water mixtures were separated. For EtOH and PrOH there was not a significant difference for the two designs both for the separation factors and fluxes. However, for MeOH both the selectivity and the flux observed in the cross flow system was about two times larger than in the dead-end system. MeOH which has the highest mobility was affected more than the mass transfer boundary layers when compared with EtOH and PrOH. Mixing the feed solution decreases mass transfer limitations.

The **support material** of the membrane influences the separation factors in pervaporation. It is observed that membranes prepared on stainless steel supports exhibit much higher separation factors than the ones prepared on alumina supports [40, 41, 48]. For membranes prepared on alumina supports, although no aluminum source is used in synthesis solution due to aluminum leaching from support; aluminum incorporates into the zeolite framework. When aluminum incorporates into the framework in place of silica a charge balancing cation is required since aluminum is trivalent. The negatively charged framework and positively charged cations result in electrostatic poles attracting polar molecules. The aluminum

incorporation to the framework increases the hydrophilicity of the zeolite, decreasing the separation factor for organic/water mixtures.

Presence of **non-zeolite pores** in the zeolite films has a significant effect on pervaporation flux and separation factor. For non-zeolite pores larger than zeolite pores the faster molecule in the mixture can pass the slower molecule regarding of membranes selective property to any of these components. Moreover, Si-OH groups in non-zeolite pores introduce hydrophilic properties to the zeolite [53-55]. Tabaka et al. [53] reported a molecular simulation study for ethanol removal from water by a single silicalite crystal. Although no water permeated through the zeolite pores, there were adsorbed water molecules on silanol groups. Presence of silanol groups in non-zeolite pores decreases the separation factor in MFI membranes. For A type membranes presence of silanol groups in defects is not a problem since zeolite A is also hydrophilic. This property of silanol groups is a big contribution to zeolite A membranes separation factors for water over organics together with molecular sieving property. A zeolite A membrane can exhibit good separation factors for water/organic separations even with defects. In a study of Okamoto et al. [37] zeolite A membranes had H<sub>2</sub>/SF<sub>6</sub> selectivities near Knudsen selectivity indicating that the membranes have non-zeolite pores larger than zeolite pores; however the water/propanol selectivity was still 18,000.

The presence of non-zeolite pores can be detected by measuring fluxes of probe molecules by pure component pervaporation. Pure component pervaporation mainly serves as a characterization of a membrane's quality [2]. For a membrane with few non-zeolite pores single-component pervaporation fluxes is expected to decrease with increasing kinetic diameter. Pure component pervaporation fluxes can also be used for a rough estimation of the dimensions of the non-zeolite pores. Appreciable fluxes of molecules that are significantly larger than zeolite pores indicate flow through non-zeolite pores. H<sub>2</sub>O, MeOH, EtOH, PrOH, acetone, DMB, xylene, TIPB fluxes are measured to characterize the zeolite membranes.

## CHAPTER 3

### EXPERIMENTAL METHODS

#### 3.1. Membrane synthesis

##### 3.1.1. Materials

MFI type zeolite membranes were synthesized from clear solutions with a molar composition of  $80\text{SiO}_2:16\text{TPAOH}:1536\text{H}_2\text{O}$ . The materials used for the preparation of synthesis solutions were LUDOX AS-30 (Aldrich), tetrapropylammonium hydroxide (TPAOH, Acros) and demineralized water.

Membranes were synthesized on  $\alpha\text{-Al}_2\text{O}_3$  and  $\gamma\text{-Al}_2\text{O}_3$  tubes obtained from Pall Exekia. The length of the tubes was 4.5 cm with an inner diameter of 0.7 cm and a wall thickness of 0.15 cm. The average pore size on the inner surface of tubes was 200 nm for  $\alpha\text{-Al}_2\text{O}_3$  and 5 nm for  $\gamma\text{-Al}_2\text{O}_3$ . Before synthesis, the tubes were washed with water in ultrasonic bath for 10 min, and then washed with 0.1 M  $\text{HNO}_3$  solution; followed by rinsing and drying. To create non-porous ends about 1 cm, the porous supports were glazed with Duncan IN1001 Envision Glaze, leaving an effective membrane permeation area of  $5.5\text{ cm}^2$ .

##### 3.1.2. Membrane seeding

Before membrane synthesis the tubular supports were seeded by dip coating as shown in Figure 3.1.

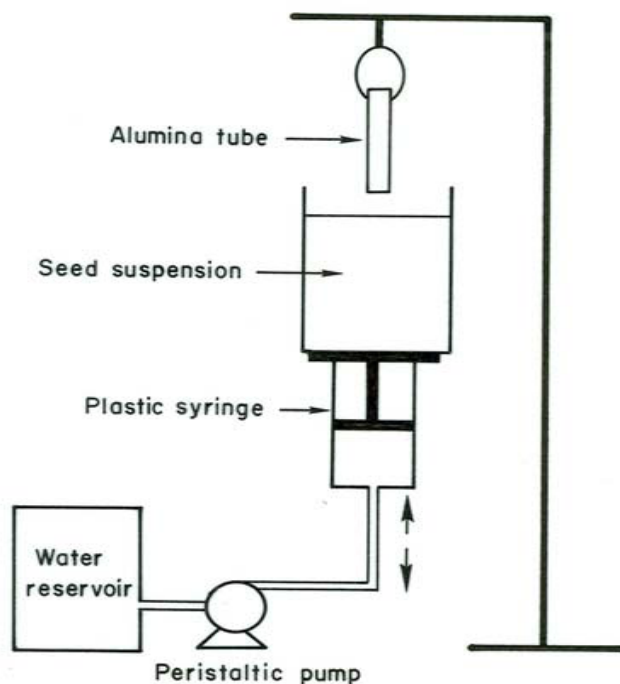


Figure 3.1. Schematic drawing of the dip-coating set-up [82]

The seed suspension is 0.25 wt% aqueous suspension of ZSM-5 and the seeds were synthesized by using a batch composition of 1.0TPAOH:8.17SiO<sub>2</sub>: 0.08Na<sub>2</sub>O:162.09H<sub>2</sub>O: 32.68C<sub>2</sub>H<sub>5</sub>OH. A beaker of 100 ml is filled with seed suspension and placed on the top of a plastic syringe of 60 ml. The support material is placed vertically at a constant level. The plastic syringe is connected to a peristaltic pump with silicone tubing as piping. Water from a reservoir is pumped to the plastic syringe so the syringe and therefore the beaker move upwards with a velocity around 1-1.5 cm/h and the support is immersed into the seed suspension. When the support fully enters to the suspension, one glazed end may stay outside; the pump is closed for 10 minutes. After this, the water is pumped from the syringe to the reservoir so the beaker moves downwards with the same velocity. When the support is removed from the suspension, it is turned upside down and the same process is repeated once

more to have a uniform coating on the support. To adhere the seeds to the surface, supports were kept at 150 °C for 4 hours.

### **3.1.3. Membrane synthesis in the recirculating flow system**

Synthesis was carried out in the recirculating flow system in which the synthesis solution is recirculated through the membrane support. A schematic of flow system is given in Figure 3.2.

Figure 3.2. Schematic of the recirculating flow system used for membrane synthesis [81]

Synthesis solution is kept in a 100 ml reservoir made of glass. Reservoir has four entries; two of these are for the streams entering and leaving the reservoir, one is for condenser connection and the other one is present to enable sample taking during operation. The streams leaving and entering to the reservoir are connected to the two ends of the membrane module. The membrane was held vertically inside the glass module. A peristaltic pump is used for circulation of the synthesis solution. All the piping is platinum cured silicone tubing since it is resistant to high temperature and alkalinity.

In order to have uniform temperature a silicon oil bath is used. The reservoir, membrane module and part of the silicone tubing stay in the oil bath during synthesis. A thermometer is inserted to the oil bath to measure temperature. The silicone oil bath is on the top of a magnetic stirrer and the synthesis solution is mixed mildly.

The synthesis solution has a molar composition of  $80\text{SiO}_2:16\text{TPAOH}:1536\text{H}_2\text{O}$ . Ludox is used as the silica source. Before membrane synthesis the synthesis solution is aged for 24 h by stirring vigorously. The module, reservoir, and the pump were connected by the tubing first, then the solution was poured into the reservoir and inserted into the silicon oil bath preheated up to the synthesis temperature. Condenser was placed on the top of the reservoir. Synthesis was done at  $95\text{ }^\circ\text{C}$  at a flow rate of 6 ml/min for a duration of 72 hours. Before synthesis the initial level of the solution in the reservoir was marked to check during synthesis. Deionized water was added to the solution from the top of the condenser when the level of solution was below the initial level of solution by assuming that only water loss takes place by evaporation. The loss by evaporation was small, few milliliters of deionized water was added daily to keep the level constant which corresponds to 5-10 ml total deionized water addition for a three days synthesis period. After synthesis, membranes were washed with distilled water until the pH of wash-water dropped around 8, and dried overnight at  $80^\circ\text{C}$ .



### **3.1.4. Membrane synthesis in the batch system**

The support was placed vertically in a polytetrafluoroethylene (PTFE) insert filled with synthesis solution. The synthesis solution has the same composition and aging conditions as in the flow system. The PTFE cap was inserted into an autoclave and the autoclave was placed into an oven preheated to 95 °C. Synthesis takes place for a duration of 72 h similar to the synthesis in the flow system. Membranes were washed with distilled water and dried overnight at 80 °C.

### **3.2. Template removal and initial characterization**

After drying a membrane, the N<sub>2</sub> permeance was measured before the removal of the organic template. A membrane without defects is likely to be impermeable in order to be considered as a high quality membrane [49]. Only the impermeable uncalcined membranes were used for pervaporation and gas permeation experiments. If the membrane had a gas permeance before removal of the template after first synthesis, an additional second layer was synthesized so that the membrane had no N<sub>2</sub> permeance before template removal.

For the removal of the organic template membrane was calcined at 450 °C for 8 h. The membrane was heated at a rate of 0.6°C/min. Temperature was kept constant at 450 °C for 8 hours and membrane was cooled to room temperature. Heating and cooling rates were slow to minimize the possibility of crack formation due to the thermal incompatibility between  $\alpha$ -Al<sub>2</sub>O<sub>3</sub> and MFI.

### 3.3 Membrane Characterization

For phase identification membranes were characterized by Philips PW 1729 X-ray diffractometer. Operating conditions are given in Table 3.1. To have the X-ray micrographs of the inside of the tubular supports, the support was broken into small pieces and placed onto the holder.

Table 3.1. Operating conditions of the X-ray diffractometer

Tube	Cu
Filter	Ni
Radiation	CuK $\alpha$
Voltage (kV)	40
Current (mA)	30
Speed ( $^{\circ}2\theta/s$ )	0.1
Time Constant (s)	1
Slit (mm)	0.2

JEOL JSM-6400 Scanning Electron Microscope (SEM) was used for morphology determination. The samples for surface and cross-section micrographs were coated with gold before analysis.

#### 3.3.1. Measuring single gas permeances

Single gas permeances of N<sub>2</sub>, H<sub>2</sub>, CO<sub>2</sub>, CH<sub>4</sub>, SF<sub>6</sub>, n-C<sub>4</sub>H<sub>10</sub> and i-C<sub>4</sub>H<sub>10</sub> were measured in a dead-end module by creating a pressure difference of 1 bar across the membrane. The permeate side was kept at atmospheric pressure, 0.91 bar and the permeate flow rate was measured by a bubble flow meter.

A schematic of the single gas permeation set-up is given in Figure 3.3. Temperature was varied between room temperature and 200°C. O-rings used for sealing the membrane to the module cannot function properly above 200°C. The transmembrane pressure difference was between 1 and 1.2 bar.

The permeance was calculated by dividing the molar flow rate to the pressure difference across the membrane and effective permeable membrane area as shown in equation 3.1. The molar flow rate is calculated from the measured volumetric flow rate by simply using the ideal gas law.

The ideal selectivity was defined as shown in equation 3.2.

Figure 3.3. Schematic of the single gas permeation set-up [82]

### **3.2. Pervaporation**

Pervaporation experiments were carried out in a cross-flow system as shown in Figure 3.4. The pervaporation system operated continuously and the feed mixture was circulated around the membrane module. The pervaporation unit consists of two parts, feed and permeate sides.

Figure 3.4. Schematic drawing of the pervaporation set-up

### ***Feed side***

The feed side consists of feed tank, membrane module, thermocouple and centrifugal pump. Membrane was sealed to the membrane module by silicone O-rings. The feed stream was circulated through the membrane module for the minimization of the mass transfer limitations with a centrifugal pump operating at a flow rate of 400 ml/min. All piping in the feed side is stainless steel, the feed tank is glass. The feed tank has a volume of 400 ml. This volume was selected so that the effect of selective permeation from the membrane would have a negligible effect on feed concentration. 300 ml of the feed tank was filled with feed solution; 100 ml empty space was left. Ethanol/water, 2-propanol/water and acetone/water mixtures of 5 wt % organic were separated by pervaporation. Also pure alcohol and water fluxes were measured for some membranes.

All piping in the feed side, including the membrane module and the feed tank was electrically heated for operations at elevated temperatures. A heating tape was rounded on the feed side and the tape was connected to a temperature controller. A thermocouple was installed on the feed side of the membrane module to measure the feed temperature. Feed temperature was varied between 25 °C-85 °C for organic/water mixtures and pure water. For pure alcohol, pervaporation measurements were carried out between 25 °C-65 °C. No variation in temperature was observed during the pervaporation experiments with time.

### ***Permeate side***

The permeate side consists of a pressure gauge, vacuum pump and three liquid nitrogen traps. The vacuum pump was used to provide the driving force for permeation. The pressure of the permeate side was kept constant at 0.34 kPa absolute in all operations. The pressure was measured by a pressure gauge placed after the

membrane module in the permeate side. To condense the permeate stream in vapor phase, two liquid nitrogen traps were used. At the exit of the two parallel traps, a safety trap was used to condense uncaptured vapor in the previous trap.

All piping in the permeate side including traps and valves are made of glass except the connections for membrane module and the pressure gauge. The glass parts are shown by gray lines and the stainless steel parts are shown by black lines in Figure 3.4. Glass was preferred instead of stainless steel for permeate side because adsorption on glass surface is less when compared with steel surface. To connect glass piping to glass traps heat shrink tubing was used. To connect the glass piping to steel piping ultra-torr cajon fittings resistant to high vacuum provided by Swagelok were used.

#### ***Operation of the pervaporation set-up***

To operate the pervaporation system, first vacuum is established in the permeate side. The pressure drops to 0.34 kPa absolute in a few minutes. When the pressure drops to the desired value, liquid N<sub>2</sub> was poured into the safety trap. After this step the centrifugal pump was switched on to circulate the feed solution around the membrane and liquid nitrogen was poured into one of the parallel traps to collect the permeate sample.

The permeate side consists of two parallel lines to enable continuous operation. When one line is in operation the other one is not. This flexibility allows sample taking from one line while the other line is in operation. A three-way valve was used to give the desired direction to flow. The permeate flow was directed to any one of the parallel lines, one line was kept in vacuum while the other one was open to atmosphere. Each line was operated for one to two hours to collect the permeate sample. The time required for collecting the permeate sample depended on

membranes flux. One or two hours of operation for each line was usually enough to collect an appreciable amount, however for membranes with two layers the operation lasted for four to five hours at room temperature. When the sample was collected, the other line was put into operation by simply changing the direction of flow using the three way valves. The line in which the permeate sample was collected was opened to atmosphere, by the use of a two-way valve. By this way, the sample was collected in one line while the other line was still in operation.

The composition of the permeate side was analyzed with Varian CP-3800 Gas Chromatograph with a Porapak T Column and a thermal conductivity detector. The operating parameters of the gas chromatograph are given in Table 3.2. No measurable amount was collected in the third safety trap, so only the samples collected in the parallel two traps were taken into account for the flux and selectivity determination.

Table 3.2. Operating conditions for the gas chromatograph

Column	Porapak T
Column Temperature	150 °C
Valve Temperature	150 °C
Detector	TCD
Detector Temperature	180 °C
Reference Flowrate	69 mol/min
Column pressure	30 psi

The flux of the membranes were calculated by simply measuring the amount of permeate collected in a certain time. The calculation of separation factor and flux is given in literature survey part. The selectivity and flux values of the permeate



samples were accepted as the steady state values only when the deviation of both was within a range of 5% from the previous sample. The variation of fluxes and selectivities with time are given in Appendix C.

The composition of the feed solution was checked and feed was refreshed to keep the feed composition constant when necessary. No change was observed in concentration for measurements at low temperatures. However, at high temperatures organic percent decreased due to evaporation of the organic compound. Feed solution was refreshed once in 2-3 hours for operations at high temperatures.

When the feed mixture was refreshed, system was free from the compounds of the previously separated mixture. The new feed mixture was poured into the feed tank, circulated, and then disposed. Usually this step was repeated 1-2 times more to clean the feed side totally until different components from the previous mixture was not detected. The permeate side was kept under vacuum for 3-4 hours to get rid of the previously adsorbed species. Any remained specie from previous experiments could be detected during analysis by gas chromatograph.

Leak tests were performed under vacuum before beginning the pervaporation experiments and repeated once in every month to make sure that the system works properly. In these tests, a non-porous tubular support was inserted to the membrane module so that the connection of the permeate side to the feed side was blocked. Then the vacuum pump was operated for 1-2 hours, the three way valve was closed to the direction of the vacuum pump, and the pump was closed. Therefore all the permeate side was kept under vacuum. Any leak in the system could be detected by an increase in the permeate pressure. The system was left under vacuum overnight to make sure that no leak was present in the system.

## CHAPTER 4

### RESULTS AND DISCUSSION

#### 4.1. Characterization of membranes

Table 4.1 shows the synthesis conditions of membranes. All membranes were seeded with 300-nm-sized MFI crystals by dip-coating. Crystallization was carried out both in a recirculating flow system and in a batch system for a duration of 72 h at 95 °C. The synthesis solution, temperature and time were the same for both methods. Some of the membranes (F2, F3, F4 and B2) were subjected to consecutive syntheses steps to eliminate the nonzeolitic pores indicated by N<sub>2</sub> permeance before calcination.

Table 4.1. Synthesis method, number of synthesis steps and N<sub>2</sub> permeances before calcination for the MFI membranes

Membrane	Synthesis Method	Number of synthesis steps	N <sub>2</sub> permeances before calcination (mol/m <sup>2</sup> .Pa.s)	
			After first synthesis	After second synthesis
F1	Flow	1	<10 <sup>-12</sup>	-
F2	Flow	2	<10 <sup>-12</sup>	<10 <sup>-12</sup>
F3	Flow	2	10 <sup>-8</sup>	<10 <sup>-12</sup>
F4	Flow	2	10 <sup>-7</sup>	<10 <sup>-12</sup>
B1	Batch	1	<10 <sup>-12</sup>	-
B2	Batch	2	10 <sup>-8</sup>	<10 <sup>-12</sup>

XRD patterns of the residual powder remained after synthesis is used as an indication of the phase grown on the support [60, 61]. Besides, XRD characterization of the residual powder enables identification of the phase without breaking the membrane. In Figure 4.1, XRD patterns of the residual powders remained after the first and second syntheses are shown for F3. Peak positions and intensities indicate highly crystalline MFI structure in the residual powder for both syntheses, which also indicate presence of MFI structure on the support. The yield of the synthesis composition was 70 %.

Figure 4.2 shows the XRD patterns of the surfaces of membranes F3 and B2. The XRD patterns indicate that the only crystal phase grown on the alumina support was MFI type zeolite. The relatively low MFI peak intensities compared to alumina peak intensities are also encountered for thin MFI type membranes in the literature [29, 58, 64].

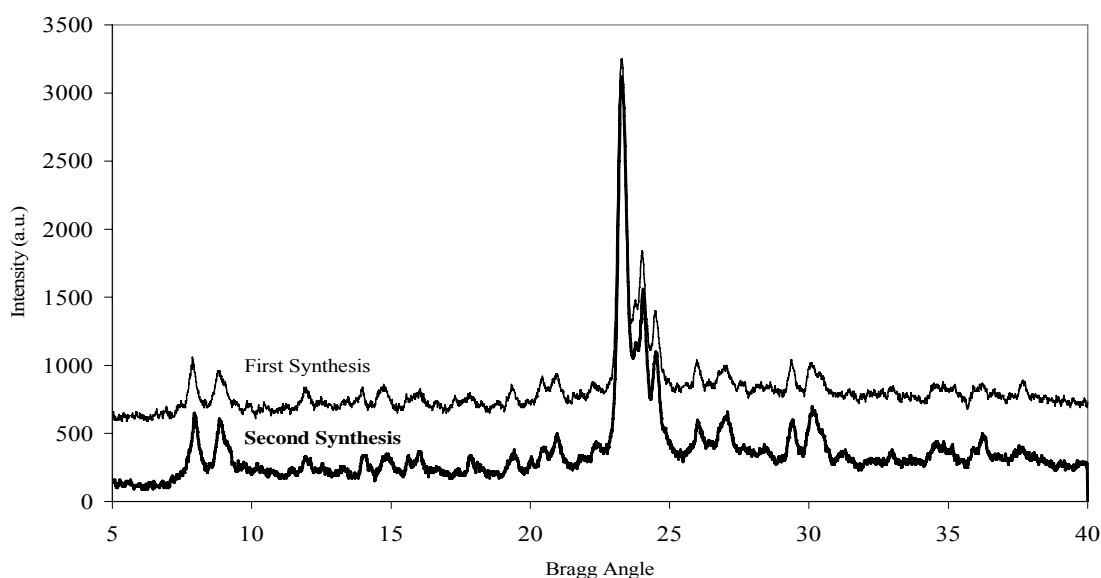


Figure 4.1. XRD patterns of the residual powders obtained after membrane synthesis F3: flow system, two synthesis steps

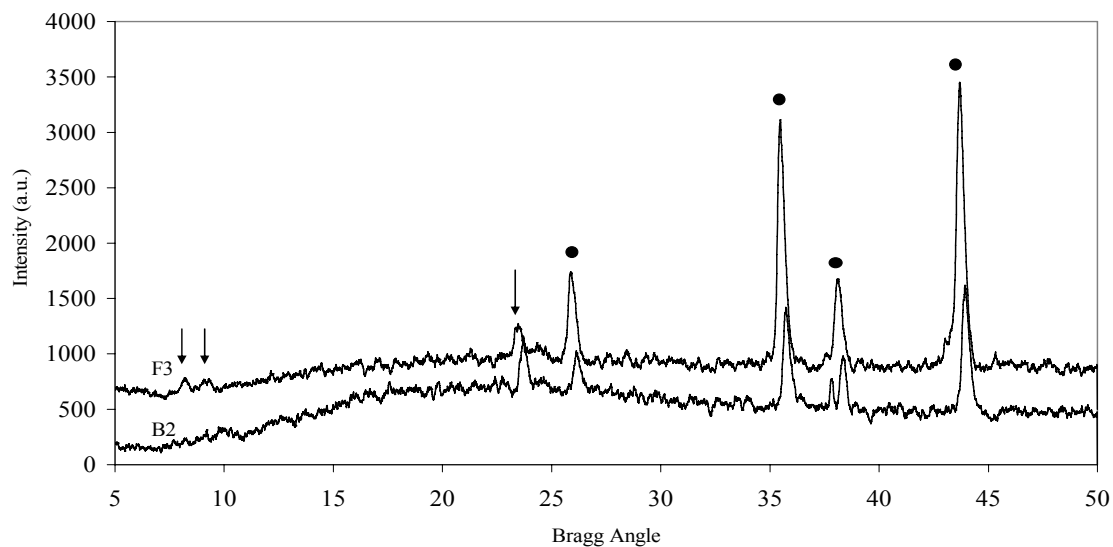
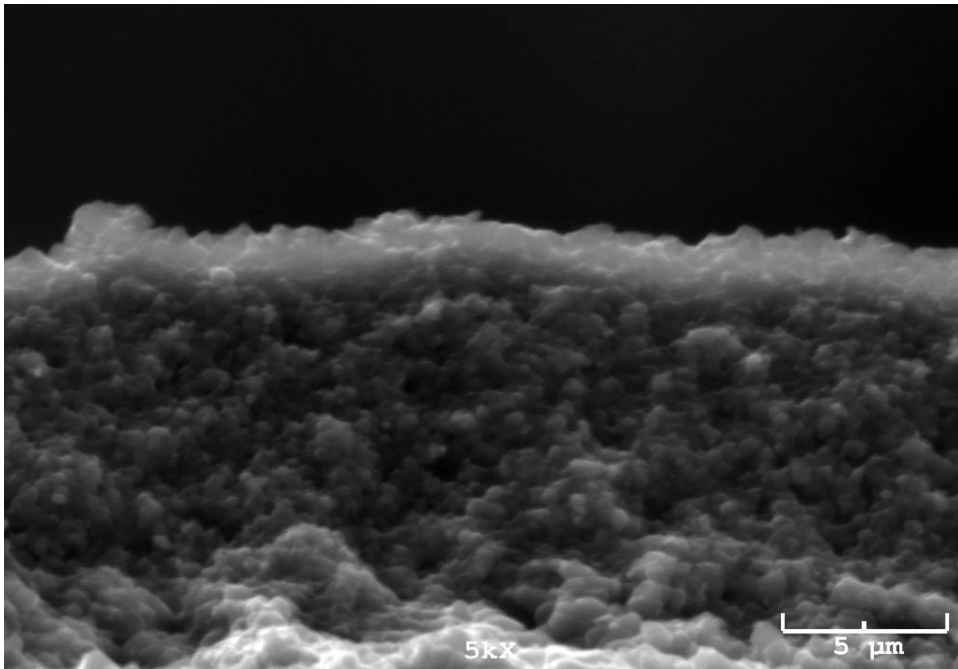


Figure 4.2. XRD patterns of membrane surfaces for membranes F3 and B2. F3: flow system, 2 synthesis steps; B2: batch system, 2 synthesis steps (arrows represent MFI peaks and dots represent alumina peaks)

The SEM cross-section micrographs of membranes F3 and B2 are shown in Figure 4.3. From the SEM micrographs the continuous and thin MFI layers on porous supports can be clearly seen. The thicknesses of both membranes are approximately 2  $\mu\text{m}$ . In Figure 4.4 the SEM micrographs of the inner surfaces of membranes F3 and B2 are shown. The crystals forming the membranes are globular in shape. When membranes F3 and B2 are compared, the deposition of crystals is less for membrane F3. During the synthesis in the flow system, the settling of zeolite particles from bulk solution is expected to be less when compared with synthesis in the batch system. Therefore synthesis in a flow system can yield more uniform membranes, free of settled crystals from the bulk.

(a)



(b)

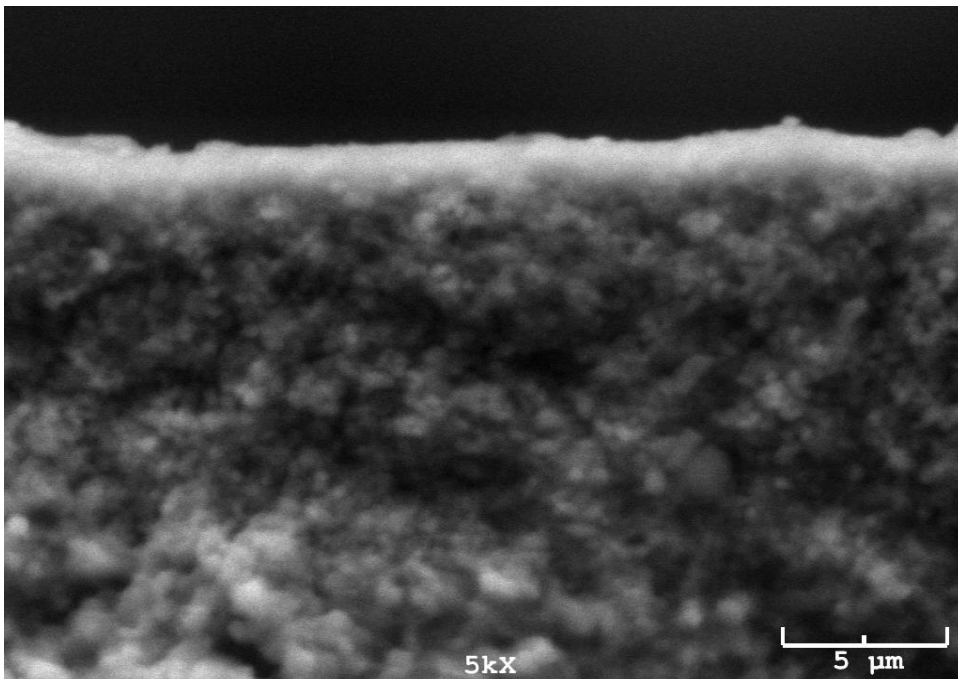
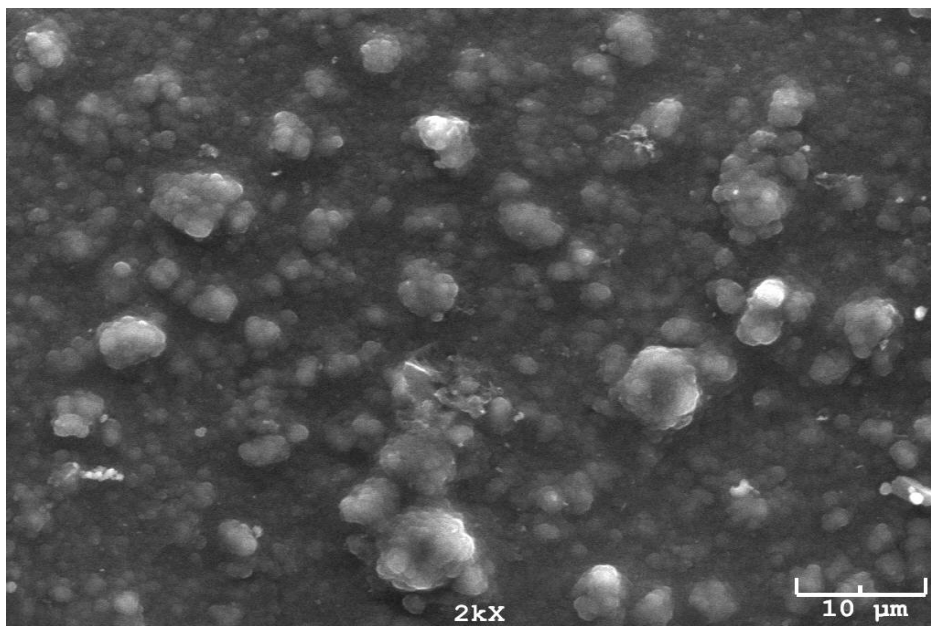


Figure 4.3. Cross-section micrographs of membranes (a): F3: flow system, two synthesis steps; (b): B2: batch system, two synthesis steps

(a)



(b)

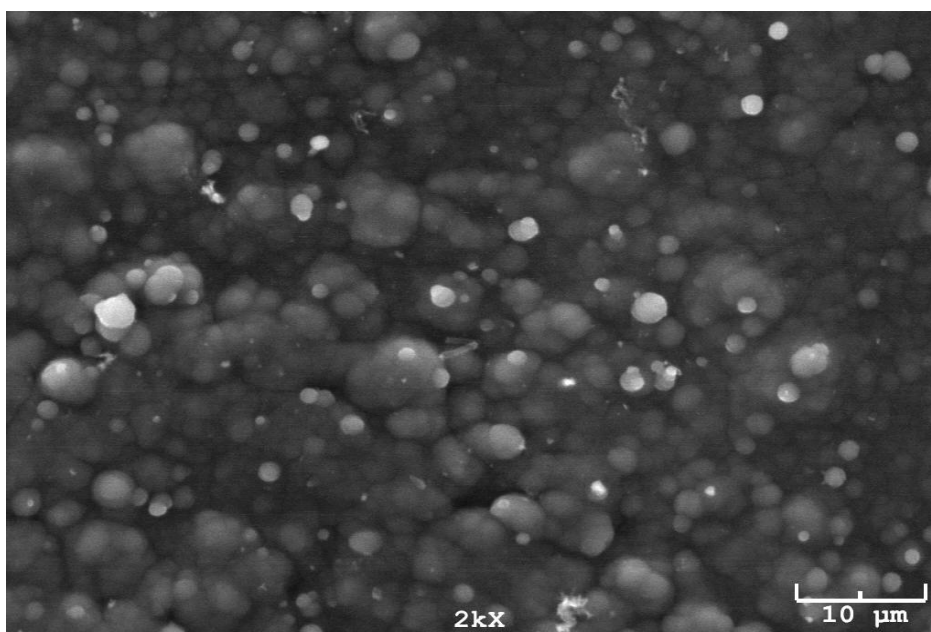


Figure 4.4. Surface micrographs of membranes (a):F3: flow system, two synthesis steps; (b): B2:batch system, two synthesis steps

## 4.2. Single gas permeances before calcination

Template molecule, TPAOH, used in the membrane synthesis occupies both the MFI pores and the small non-zeolitic pores in the intercrystalline boundaries. Therefore a membrane is expected to be impermeable to small molecules if no large defects are present [49]. Table 4.1 shows the N<sub>2</sub> permeances before calcination. Membranes F1, B1 and F2 were impermeable to N<sub>2</sub> after the first synthesis. Membranes F3, F4 and B2 on the other hand had N<sub>2</sub> permeances in the order of magnitude of 10<sup>-8</sup> mol/m<sup>2</sup>.Pa.s after the first synthesis indicating that these membranes had defects. The possible reasons to these defects in our thin membranes might be insufficient seeding, problems in the crystal growth or problems on the support surface such as impurities. A second layer was crystallized onto these membranes to eliminate the defects in the first layer. This technique is commonly applied to prepare defect free membranes indicated by gas permeance before calcination [58, 65]. All membranes became impermeable to N<sub>2</sub> after the synthesis of a second layer. Consecutive syntheses can reduce the number and size of the defects on membrane surface.

## 4.3. Single gas permeances after calcination

Figure 4.5 shows the single gas permeances of H<sub>2</sub>, N<sub>2</sub>, CO<sub>2</sub>, CH<sub>4</sub>, n-C<sub>4</sub>H<sub>10</sub> and i-C<sub>4</sub>H<sub>10</sub> through MFI membranes as a function of the kinetic diameter of the permeating molecule. Measurements were carried out at 25 °C and 200 °C. All membranes, regardless of the synthesis method, exhibited similar behavior. The permeances of H<sub>2</sub>, N<sub>2</sub>, CO<sub>2</sub> and CH<sub>4</sub> which are smaller than channels of MFI showed greater permeances than the permeance of i-C<sub>4</sub>H<sub>10</sub>, whose size is comparable to the size of MFI channels, suggesting that the membranes have only few defects.

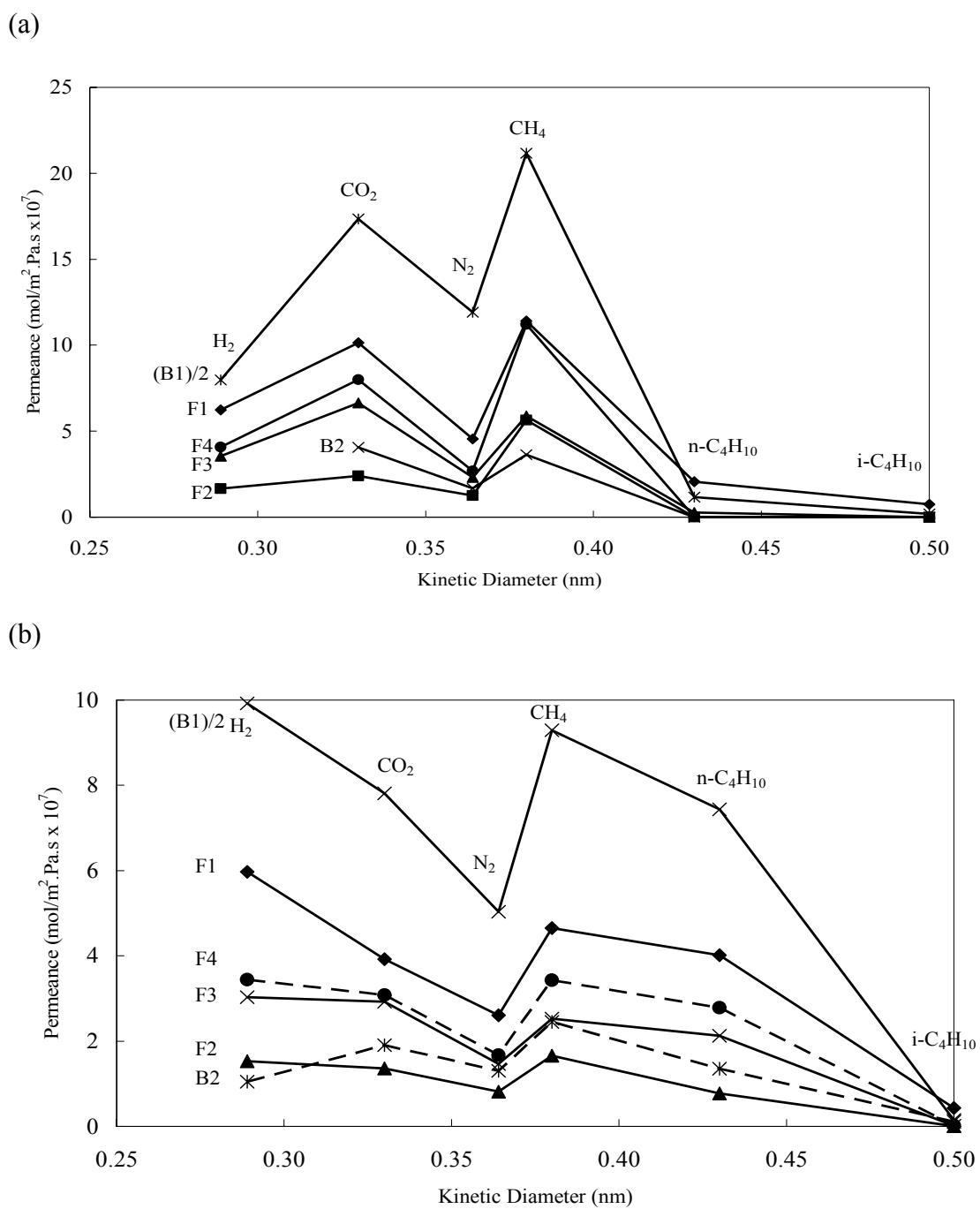


Figure 4.5. Single gas permeances as a function of kinetic diameter for the MFI membranes (a): at 25 °C; (b): at 200 °C



Figure 4.5-a shows single gas permeances at 25 °C. The fastest permeating gas was CH<sub>4</sub> although it is larger than N<sub>2</sub>, CO<sub>2</sub> and H<sub>2</sub>; CO<sub>2</sub> permeated faster than H<sub>2</sub> although CO<sub>2</sub> is larger than H<sub>2</sub>. The larger molecules can permeate faster than smaller molecules if they adsorb more strongly (Heat of adsorption for CH<sub>4</sub>:16.4 kJ/mol [63]). Apparently membranes adsorb CH<sub>4</sub> and CO<sub>2</sub> more strongly than the H<sub>2</sub> and N<sub>2</sub> at 25°C because H<sub>2</sub> and N<sub>2</sub> are expected to diffuse through MFI pores faster than CH<sub>4</sub> due to their smaller kinetic diameter [Diffusivities are  $7 \times 10^{-7}$ ,  $5 \times 10^{-8}$  and  $1 \times 10^{-10}$  for H<sub>2</sub>, N<sub>2</sub> [62] and CH<sub>4</sub> [56] respectively].

Figure 4.5-b shows the single gas permeances at 200 °C. The permeances of N<sub>2</sub>, CO<sub>2</sub> and CH<sub>4</sub> decreased with temperature because the adsorption coverages decreased at 200°C although their diffusivities increased [66]. The coverages of weakly adsorbing gases are expected to be lower at 200°C than 25°C because adsorption is exothermic. In contrast, n-C<sub>4</sub>H<sub>10</sub> permeance increased significantly with temperature so that it became comparable to the permeances of weakly adsorbing gases. No significant change was observed for the permeances of i-C<sub>4</sub>H<sub>10</sub> with temperature [67].

Regardless of the synthesis method, flow or batch, the membranes with two layers had significantly lower permeances than the membranes with one layer. For butane isomers the decrease in permeance with consecutive synthesis was more drastic so that the n-butane permeances through membranes with single layer were 10 times as high as n-butane permeances through membranes with two layers. The lower permeances with increase in the number of synthesis steps can be attributed to the plugging of the nonzeolitic pores [68] or to the increasing thickness of the membranes. The SEM images of membranes synthesized as single layer [membrane F3, which was synthesized with the same procedure, 17] and as two layers [membrane F3, this work], however, revealed that there is no significant difference in thicknesses, suggesting that the decrease in permeances with consecutive synthesis is because consecutive synthesis mainly patched the membrane layer to eliminate the nonzeolitic pores.

The ideal selectivities shown in Table 4.2. also suggest a similar conclusion. The  $H_2/n-C_4H_{10}$ ,  $CH_4/n-C_4H_{10}$ ,  $n-C_4H_{10}/i-C_4H_{10}$  ideal selectivities increased with the number of synthesis steps for membranes synthesized in the flow system. The ideal selectivities for membranes synthesized in the flow system with two layers are 13-18 times higher than the quality criteria (10) postulated by Vroon et al. [58] for butane isomers. The increase in ideal selectivities with consecutive synthesis showed that consecutive synthesis effectively sealed the intercrystalline voids.

Table 4.2. Ideal gas selectivities of  $n-C_4H_{10}/iso-C_4H_{10}$ ,  $H_2/n-C_4H_{10}$ , and  $CH_4/n-C_4H_{10}$  gas pairs through MFI membranes at 25°C and 200°C

Gas Pair	$n-C_4H_{10}/iso-C_4H_{10}$		$CH_4/n-C_4H_{10}$		$H_2/n-C_4H_{10}$	
	25°C	200°C	25°C	200°C	25°C	200°C
<b>F1</b>	2.8	8.8	5.5	1.2	3.0	1.5
<b>F2</b>	1.3	131	1263	2.1	370	2.0
<b>F3</b>	112	180	21.5	1.2	12.9	1.4
<b>F4</b>	6.7	139	560	1.2	204	1.2
<b>B1</b>	6.1	50	18.2	1.2	6.9	1.3
<b>B2</b>	1.0	12.2	558	1.8	-	0.8
<b>Knudsen</b>	<b>1</b>		<b>1.9</b>		<b>5.4</b>	

For membranes synthesized in the batch system, the ideal selectivity for  $CH_4$  over  $n-C_4H_{10}$  increased with the increasing number of synthesis steps similar to membranes prepared in the flow system. However, the ideal selectivity for  $n-C_4H_{10}$  over  $i-C_4H_{10}$  unexpectedly decreased, indicating that membranes have still non-zeolitic pores even after synthesis of second layer or new defects formed during the calcination to vacate MFI pores.

$n\text{-C}_4\text{H}_{10}/i\text{-C}_4\text{H}_{10}$  ideal selectivity strongly depends on the large non-zeolitic pores in a membrane. Non-zeolitic pores, which are essentially in mesoporous region, cannot separate isomers because Knudsen diffusion governs the permeation in mesopores. Knudsen selectivity, which is related to the square root of the ratio of molecular weight of diffusing molecules, is equal to one for isomers. Therefore, a zeolite membrane exhibiting high  $n\text{-C}_4\text{H}_{10}/i\text{-C}_4\text{H}_{10}$  ideal selectivity can be evaluated as good quality, as suggested by Vroon et al. [58], who considered that MFI membranes with  $n\text{-C}_4\text{H}_{10}/i\text{-C}_4\text{H}_{10}$  ideal selectivity of greater than 10 were of high quality.

Among membranes synthesized by consecutive synthesis (F2, F3, and B2), synthesis in the flow system resulted in better ideal selectivities. The  $n\text{-C}_4\text{H}_{10}/i\text{-C}_4\text{H}_{10}$  ideal selectivities for membranes F2 and F3 were 13-18 times higher than the quality criteria postulated for butane isomers [11, 23]. The ideal selectivities for  $\text{H}_2/n\text{-C}_4\text{H}_{10}$  and  $\text{CH}_4/n\text{-C}_4\text{H}_{10}$  gas pairs were 2-69 and 12-665 times higher than Knudsen selectivity at 25°C for membranes F2 and F3. The ideal selectivities higher than Knudsen selectivities suggest that membranes synthesized in this study are of good quality. The better selectivities of membranes prepared in the flow system can be attributed to the more uniform synthesis conditions provided by the flow of the synthesis solution. Synthesis in a flow system can minimize the deposition of MFI particles from the bulk solution onto the membrane surface so that the membranes are formed from crystals grown on the support directly; which is expected to result in membranes with more uniform thicknesses. In a membrane with a non-uniform thickness, the thicker regions in the zeolite film might have more crystals and grain boundaries when compared with thinner ones. Regions with different thicknesses can have different thermal expansions and this can result in defect formation in the zeolite film during calcination. Synthesizing a membrane with a uniform thickness can reduce the stress occurred in the zeolite film during calcination; and therefore reduce the defects in the film yielding to membranes with a higher quality.

### 4.3.1. Effect of temperature on single gas permeation

The variation of single gas permeation with varying temperature was investigated for membranes synthesized in the flow system. Membrane F1, which has one layer and membrane F2, which has two layers, were selected to measure single gas permeances at different temperatures (Figure 4.6) The trends of the permeances of gases were similar for both membranes.

Permeation of gases through zeolite membranes show a minimum, maximum or both with respect to temperature; indicating that some transport mechanisms coexist [71]. It is reported in literature that transport through zeolite membranes is a combination of surface diffusion and activated gaseous diffusion [72, 73]. As the operating temperature increases the diffusivity becomes larger, enhancing the permeance. However, the adsorption equilibrium constant decreases with temperature; leading to less coverages and reduced permeances [74]. The trend of the permeance curve depends on the transport mechanism that dominates.

In literature, it is reported that a maximum is reached for permeances of CO<sub>2</sub> and n-C<sub>4</sub>H<sub>10</sub> with respect to temperature [70, 74-80]. Similar results are obtained for membranes F1 and F2. For CO<sub>2</sub> the temperature where the maximum occurs ( $T_m$ ) is less than the one for n-C<sub>4</sub>H<sub>10</sub>. It is reported that  $T_m$  increases with the adsorption strength of the molecule [77].

At temperatures where the coverage is high, the enhancement in diffusivity with temperature is dominant. The permeance increases with increasing temperature up to a certain temperature ( $T_m$ ) where the enhancement in diffusivity and reduction in coverage become comparable. At  $T_m$  a maximum occurs in the permeance curve. By further increasing the temperature, the reduction in the coverages is dominant although the diffusivity increases the permeances decrease [70, 74, 76, 77].

The  $T_m$  values are around 25-75 °C for CO<sub>2</sub> and 100-150°C for n-C<sub>4</sub>H<sub>10</sub> for our membranes. The ranges of  $T_m$  are similar to the ranges reported in literature [69, 70, 74, 78-80].

The permeance of i-C<sub>4</sub>H<sub>10</sub> did not change much with temperature. Similar results are obtained in literature [66, 67] and significant increases in permeances with respect to temperature are attributed to transport through non-zeolite pores [86]. The permeances of N<sub>2</sub> and H<sub>2</sub> are higher at low temperatures and decreases slightly with increasing temperature.

#### **4.3.2. Comparison of n-C<sub>4</sub>H<sub>10</sub> /i-C<sub>4</sub>H<sub>10</sub> selectivities with literature**

In Table 4.3, the permeances and ideal selectivities of butane isomers are compared with selectivities for MFI membranes reported in literature. Membrane synthesized by Çulfaz et al. [17] has the same synthesis parameters with membrane F1 synthesized in this work. Both membranes have one zeolite layer synthesized in the flow system. However, membrane synthesized by Çulfaz et al. [17] has n-C<sub>4</sub>H<sub>10</sub> permeance about six times larger than membrane F1 although the N<sub>2</sub> permeances are almost the same for both membranes ( $4 \times 10^{-7}$  mol/m<sup>2</sup>.Pa.s). The selectivity on the other hand is about two times higher than F1. The n-C<sub>4</sub>H<sub>10</sub> permeances of membranes F3 and F1 are almost the same, but the significantly lower permeance of i-C<sub>4</sub>H<sub>10</sub> through F3 results in a very high ideal selectivity for butane isomers for this membrane.

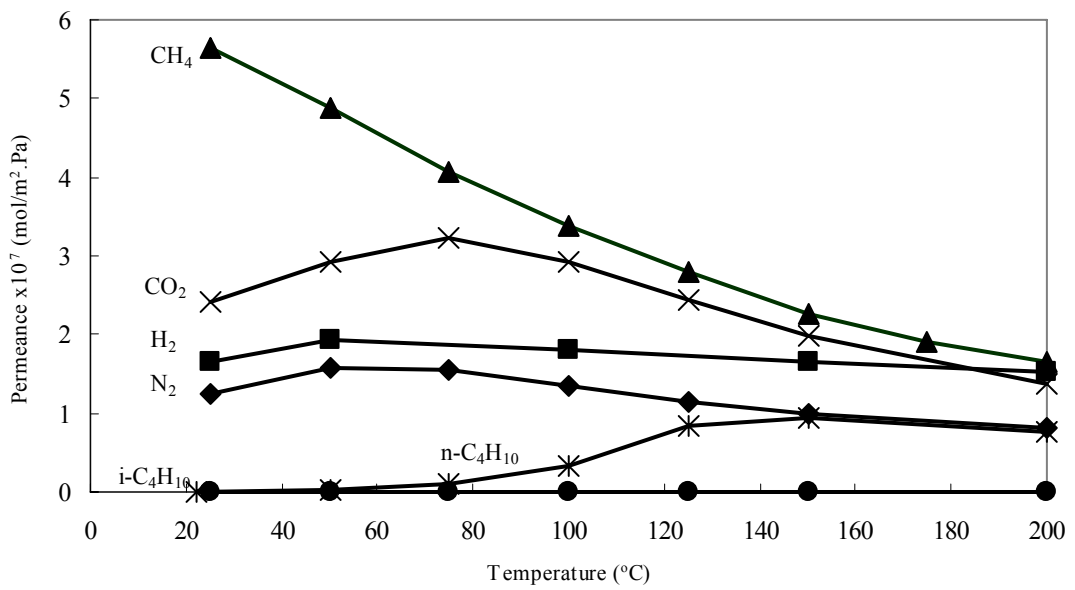
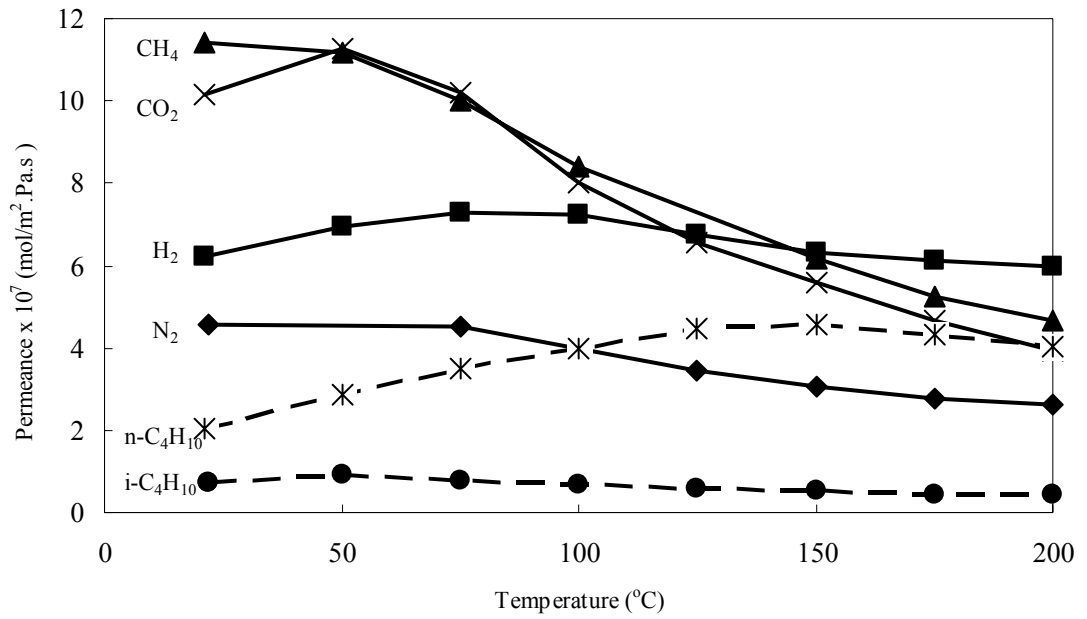


Figure 4.6. Single gas permeances as a function of temperature (a): for membrane F1, synthesized in the flow system with one zeolite layer; (b): for membrane F2, synthesized in the flow system with two zeolite layers

Table 4.3. Comparison of n-C<sub>4</sub>H<sub>10</sub> and i-C<sub>4</sub>H<sub>10</sub> permeation results with literature (at room temperature)

Author	Thickness (µm)	Permeance (mol/m <sup>2</sup> .Pa.s x 10 <sup>8</sup> )		Ideal Selectivity
		n-C <sub>4</sub> H <sub>10</sub>	i-C <sub>4</sub> H <sub>10</sub>	n-C <sub>4</sub> H <sub>10</sub> /isoC <sub>4</sub> H <sub>10</sub>
F3 (this work)	2	2.7	0.02	111
F1 (this work)		2.06	0.75	2.8
Çulfaz et al. [17]	2	16.6	2.8	5.8
Kang et al.[65]	-	9.9-29		17-39
Li et al. [38]	7	1.8	0.15	12
Hedlund et al. [67]	1.5	0.005	0.004	1.2

Kang et al. [65] synthesized MFI membranes at low temperatures like in our case. Membranes were synthesized inside the pores of alumina tubes using consecutively three or four synthesis steps at 95°C. The ideal selectivities were 17-39 for the butane isomers. Li et al. [38] reported thin and continuous ZSM-5 membranes prepared by a two step varying temperature synthesis. The permeance of i-C<sub>4</sub>H<sub>10</sub> was 0.15 x 10<sup>-8</sup> mol/m<sup>2</sup>.Pa.s and the ideal selectivity was 12. They have obtained H<sub>2</sub>/i-C<sub>4</sub>H<sub>10</sub> ideal selectivities as high as 1548.

Hedlund et al. [67] evaluated a thin ZSM-5 membrane synthesized in the absence of organic template molecules by single gas permeation. The permeances of butane isomers are significantly lower than our membranes together with a lower ideal selectivity. The lower permeance is attributed to the presence of adsorbed species in the channel system and the membrane gave a higher H<sub>2</sub>/n- C<sub>4</sub>H<sub>10</sub> ideal selectivity (99) than our membranes (1.5-13).

#### 4.4. Pervaporation separation of organic/water mixtures

MFI membranes synthesized in this study were used to separate ethanol/water, 2-propanol/water and acetone/water mixtures by pervaporation. The separation of these mixtures is widely studied because of their commercial importance and their simplicity both in analysis and in preparation [34, 38, 41, 47]. The performance of membranes in separation of alcohol/water and ketone/water mixtures was investigated. Ethanol is an alcohol with 2 carbon atoms, whereas 2-propanol is a branched alcohol with three carbon atoms and acetone is a ketone [28]. The feed composition consisted of 5 % organic and 95% water by weight. The organic amount is less than the water amount in the feed since hydrophobic MFI membranes are used to remove trace organics. 5 wt% organic compositions were selected due to plethora of experimentally published data for this composition.

Effect of synthesis parameters, number of synthesis steps and synthesis method on pervaporation selectivities and fluxes were investigated. In addition the effect of pervaporation temperature on separation factor and flux was studied. Table 4.4 shows the fluxes and separation factors for pervaporation of organic/water mixtures through MFI membranes.

Table 4.4. Separation factors and fluxes ( $\text{kg/m}^2\cdot\text{h}$ ) for pervaporation of 5 wt. % organic/95 wt. % water feed at room temperature

Membrane	EtOH/ Water		2-PrOH/ Water		Acetone/ Water	
	S.F.	Flux ( $\text{kg/m}^2\cdot\text{h}$ )	S.F.	Flux ( $\text{kg/m}^2\cdot\text{h}$ )	S.F.	Flux ( $\text{kg/m}^2\cdot\text{h}$ )
F1	16	0.3	3.4	0.7	13	0.4
F2	43	0.2	36	0.2	1024	0.1
F3	14	0.2	13	0.3	33	0.4
B1	7	1.3	5	1.2	12	1.3
B2	19	0.4	5.1	0.3	15	0.3



#### 4.4.1. Effect of number of synthesis parameters on separation factor and flux

##### *Effect of Number of synthesis steps*

Membranes with two layers had lower fluxes but slightly higher selectivities than membranes with single layer, as expected. The fluxes of membranes synthesized with two consecutive syntheses were comparable regardless of the method of synthesis.

Membrane separation factor for synthesis in the flow system was improved by additional synthesis. 2-PrOH /water separation factors were increased from 3.4 to 36 and 13, acetone/water separation factors increased from 13 to 33 and 1024. EtOH/water separation factors were increased from 16 to 43 for membrane F2, no improvement was observed for F3. The ideal selectivities for butane isomers were also increased by a factor of 13-18 with increasing number of synthesis steps. Considering both the pervaporation and gas permeation results, it can be concluded that the intercrystalline voids were successfully sealed by the consecutive layers.

For synthesis in the batch system, the separation factor was increased by a factor of 2.5 for EtOH/water mixture by increasing number of synthesis steps. No significant increase in separation factor was observed for 2-PrOH/water and acetone/water mixtures. The n-C<sub>4</sub>/i-C<sub>4</sub> ideal selectivity was 4-6 times higher for membrane with one zeolite layer. Membrane with two zeolite layers has no better ideal selectivity or separation performance but a 1/3 times less permeance. The non-zeolite pores present after the first layer indicated by N<sub>2</sub> permeance after calcination may not be sealed by consecutive synthesis or additional defects may have been introduced during calcination.

### *Effect of synthesis method*

For membranes with one layer, synthesis in the flow system resulted in a better separation factor for ethanol/water mixture while the separation factors for 2-propanol/water and acetone/water mixtures were comparable. Among membranes with one layer, the fluxes for membrane synthesized in the batch system were 2-3 times higher. For membranes synthesized by consecutive synthesis, syntheses in the flow system resulted in much better selectivities while the fluxes were comparable. The comparison of membranes synthesized in batch and flow systems in terms of flux and separation factor is consistent with the gas permeation results. The separation factors and selectivities were better for membranes synthesized in the flow system when the defects present in the first layer were sealed by additional synthesis.

#### **4.4.2. Variation of separation factor for different organics**

The separation factors were higher for acetone/water and ethanol/water mixtures; and lowest for 2-propanol/water mixture. This trend does not correlate with the relative volatilities ( $\alpha_{\text{organic/water}}$  is 10.5 for ethanol, 20.9 for 2-propanol, 42.7 for acetone [31]); 2-propanol is more volatile than ethanol but ethanol has higher separation factors. Moreover, the separation factors are much higher than ideal selectivities (Table 4.5). Therefore the separation depends on preferential adsorption of alcohols. Bowen et al. [43] reported that the separation factors correlated strongly with the organic feed fugacities in pervaporation. Two aqueous mixtures of equal compositions can have different coverages even if the heats of adsorption and molecular sizes are similar due to different fugacities. The ranking of separation factors for different organics observed in this study are consistent with the rankings observed in literature [43, 49].

#### 4.4.3 Variation of separation factor and flux with time

Figure 4.7 shows the variation of separation factor and flux with operation time for membrane F2 for acetone/water mixture separation at room temperature.

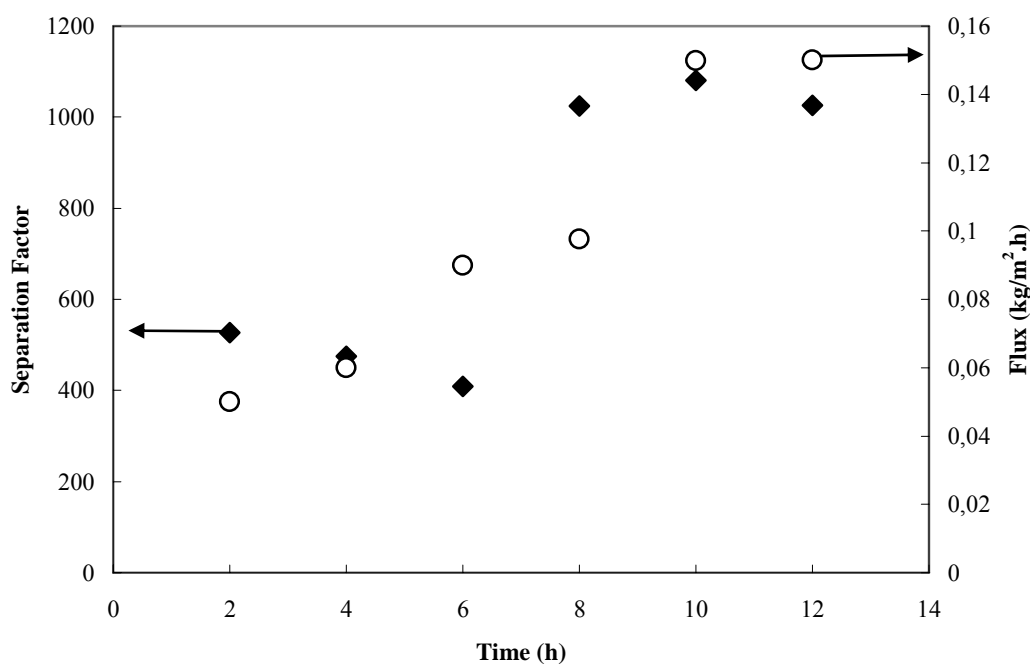


Figure 4.7. Variation of separation factor and flux for membrane F2 for 5 wt% acetone/water solution at room temperature

Both the separation factor and flux increase with time until reaching steady state. The time to reach to steady state was shorter for membranes with one layer. The trends of separation factors and fluxes are almost similar for all membranes, so the results for F2 are reported as an example. The variation of separation factor and flux with time for the other membranes is reported in Appendix C. Reported fluxes and separation factors are all steady-state values.

#### 4.4.4. Variation of separation factor and flux with temperature

The effect of temperature on separation factor and flux of membranes was investigated for pervaporation of 5 wt% EtOH/water mixtures. Figure 4.8 shows that pervaporation fluxes for the ethanol/water mixtures increase with temperature. Figure 4.9 shows the variation of separation factors with temperature for the same mixture. A slight decrease in separation factor with temperature was observed for membranes F1, F3, B1 and B2; the selectivity decreased almost 50% for membrane F2. At low temperatures ethanol blocks water permeation more effectively due to its strong adsorption. With a temperature increase the water permeation increases more than ethanol permeation increases due to lower coverage of ethanol. This results in a decrease in the separation factor. These results are consistent with results previously reported for pure silicalite membranes [14, 22, 42, 50]. Lin et al. [50] reported high quality MFI membranes with 5 wt% EtOH/water pervaporation selectivities around 90. The separation factor decreased to around 80 with increasing temperature in their case. Some researchers have reported that both the flux and the selectivity increased with temperature [31, 49]. The reason can be transport through non-zeolite pores in their cases. In another study reported for a silicalite-silicone rubber composite membrane, it was suggested that the separation factor increased with increasing temperature when the transport was through silicone rubber, and a decrease was observed in separation factor when the transport was through silicalite [13]. The variation of separation factors and fluxes in our case indicates that the transport is through zeolite pores.

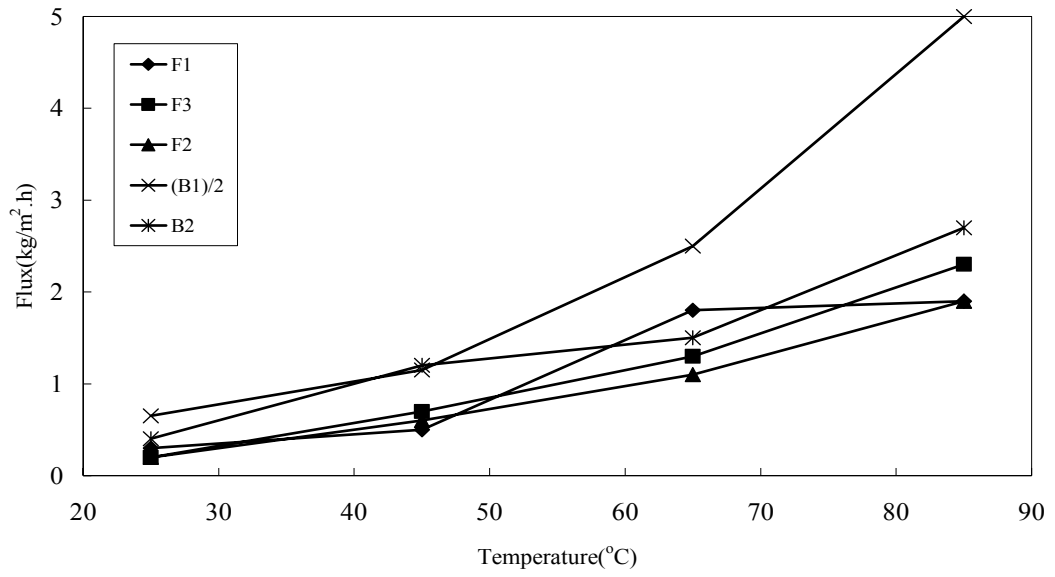


Figure 4.8. Variation of fluxes for pervaporation of 5wt% EtOH/water mixtures

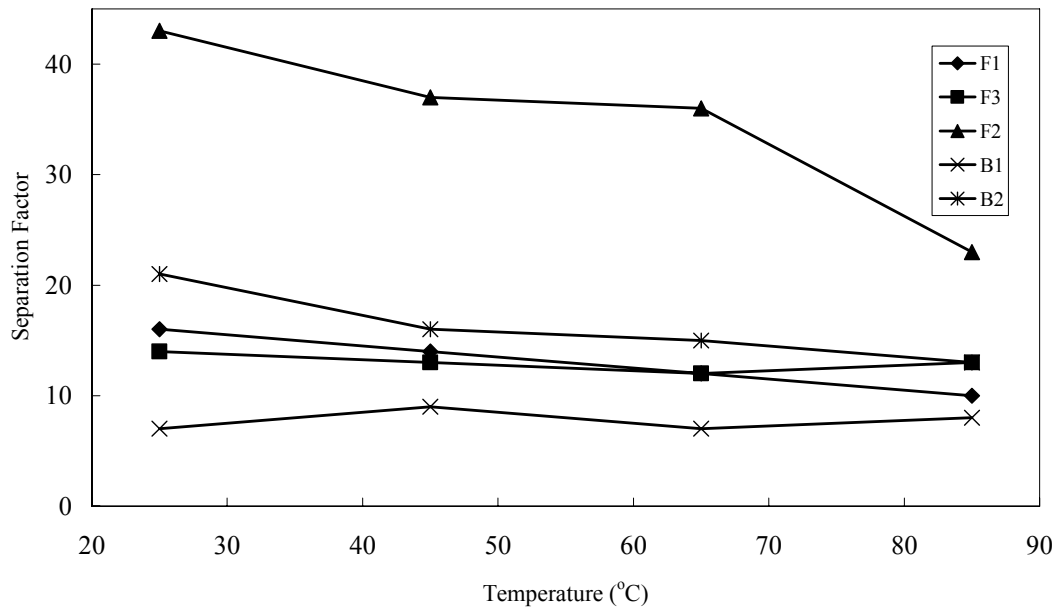


Figure 4.9. Variation of for separation factors for pervaporation of 5wt% EtOH/water mixtures

#### 4.4.5. Pure component pervaporation measurements for membrane F2

Membrane F2 which was synthesized with two consecutive syntheses in the flow system had the highest separation factors among all membranes for all organics. The ethanol/water, 2-propanol/water and acetone/water separation factors are 43, 36, 1024 respectively. The separation factors are all higher than the relative volatility for 5% organics in water (10.5 for ethanol, 20.9 for 2-propanol, 42.7 for acetone) [31]. The acetone/water separation factor is quite high yielding 98% acetone in permeate. The n-C<sub>4</sub>/i-C<sub>4</sub> ideal selectivity was also 13 times higher than the postulated quality criteria. This high quality MFI membrane was selected for further characterization, pure alcohol and water pervaporation fluxes were measured.

Figure 4.10 shows the pure water, ethanol, 2-propanol fluxes together with ethanol/water and 2-propanol/water pervaporation fluxes with respect to temperature. Fluxes of pure water, pure ethanol and 5 wt% ethanol/water mixtures through membrane F2 increased with temperature. The pure ethanol fluxes were higher than pure water and mixture fluxes; the mixture and pure water fluxes being close to each other. Table 4.5 shows the ideal and separation factors for alcohol/water mixtures.

Table 4.5. Ideal selectivities and separation factors for alcohol/water mixtures for membrane F2, synthesized with two consecutive steps in the flow system

<b>T (°C)</b>	<b>Ideal Selectivity</b>		<b>Separation Factor</b>	
	EtOH/water	2-PrOH/water	EtOH/water	2-PrOH/water
25	2.0	0.1	43	36
45	1.7	0.3	37	84
65	4.1	0.2	36	71
85	-	-	23	31

The separation factors were higher than ideal selectivities. The separation factor was 22 times the ideal selectivity at room temperature. With temperature increase the difference between the two decreased to 9, since alcohol more effectively blocked water permeation at low temperatures. The pure water fluxes were 4-10 times higher than 2-propanol fluxes. The ideal selectivities were therefore less than 1, the separation factors were 300-400 times more than the ideal selectivities. The total fluxes were comparable with pure alcohol fluxes. Ethanol had a higher permeance than propanol because larger alcohols adsorb more strongly and diffuse slower. Both organic and water fluxes decreased as the carbon number increased.

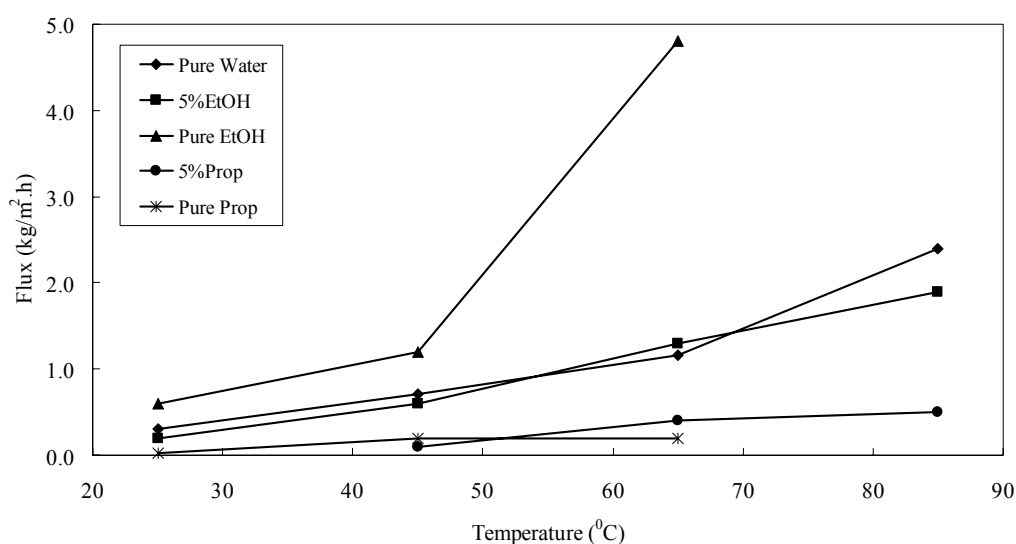


Figure 4.10. Pure water, ethanol, 2-propanol fluxes together with ethanol/water and 2-propanol/water pervaporation fluxes; with respect to temperature for membrane F2, synthesized with two consecutive syntheses in the flow system

Figure 4.11 presents water fluxes for the organic/water mixtures and pure water with respect to temperature. Water flux was reduced by presence of organics and larger

organics more effectively blocked water permeation. Water flux was decreased up to 20% of pure water flux by ethanol and 1-3% for 2-propanol and acetone. Although 2-propanol strongly inhibited water flux, it had lower separation factors than ethanol because 2-propanol permeated slower than ethanol (Figure 4.9). The diffusion mechanism dominated so the separation selectivities were lower for 2-propanol. The inhibition of water fluxes by presence of organics is typical for most MFI membranes [7, 12, 31, 49].

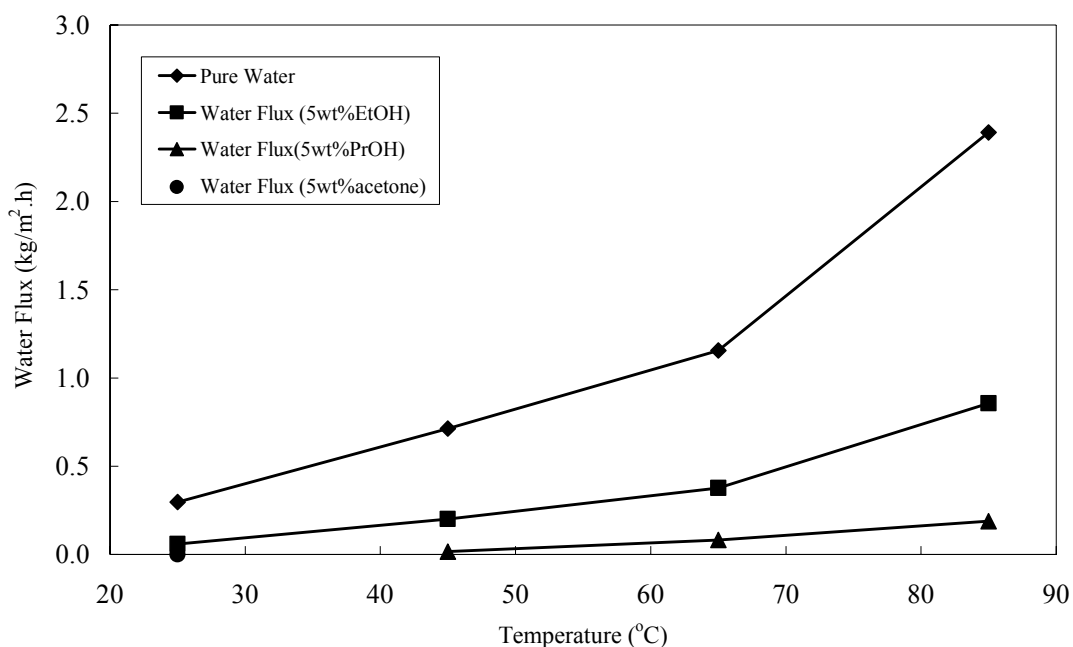


Figure 4.11. Pure water flux and water flux in presence of organics for membrane F2, synthesized with two consecutive syntheses in the flow system



#### 4.4.6. Comparison of pervaporation fluxes and selectivities with literature

The separation factors and selectivities for pervaporation separation of ethanol/water mixtures reported in literature and in this study are given in Figure 4.12. The references for this figure are given in Appendix E. The membrane performance is related to the quality of the zeolite layer; membranes with few defects are expected to show high performance in pervaporation separation of liquid mixtures. The separation of alcohol/water mixtures by MFI membranes is mainly achieved by preferential adsorption instead of molecular sieving. Therefore, the separation performance is influenced from the thickness and the Si/Al ratio of crystals forming the membrane since thick membranes adsorb more alcohol and MFI crystals become more hydrophobic as the Si/Al ratio increases. Matsuda et al. [14] reported a separation factor of 120 for ethanol/water separation, the support material was stainless steel with a disk geometry. The silicalite membranes synthesized on alumina supports on the other hand had lower selectivities due to incorporation of leached Al to the framework from the support [40, 41, 48]. Li et al. [12] reported Ge-substituted MFI membranes on SS supports with a Si/Ge ratio of 41. The isomorphous substitution was performed to increase the hydrophobicity of the silicalite membranes to improve separation factors in pervaporation. Separation factors were 47 for ethanol/water mixture, and 29 for 2-propanol/water mixture. The separation factors for these membranes were similar to the separation factors observed for membrane F2.

Most membranes in literature were grown on stainless steel supports with thicknesses between 20 [10]-400 [22]  $\mu\text{m}$ . Our membranes are 1-2  $\mu\text{m}$  thick and the effect of Al incorporation is expected to be much more significant for thin membranes. The relatively low separation factors observed for the membranes prepared in this study are probably due to lower thicknesses of the membranes and due to Al incorporation from the  $\text{Al}_2\text{O}_3$  support although they are of good quality considering the n-C<sub>4</sub>/i-C<sub>4</sub>



## CHAPTER 5

### CONCLUSIONS

In this study pervaporation separation of ethanol/water, 2-propanol/water and acetone/water mixtures were performed. Membranes were synthesized both by the flow system, where the synthesis solution is circulated through the membrane support and hydrothermal synthesis in the batch system.

Good quality thin (2 $\mu$ m) membranes were synthesized in the flow system indicated by the high ideal selectivities for butane isomers and SEM micrographs. Membranes were selective for organics over water in pervaporation separations. When the membranes synthesized in batch and flow systems are compared, the thicknesses, single gas permeances and pervaporation fluxes were found to be similar. However, for membranes synthesized by consecutive synthesis, synthesis in the flow system yielded better pervaporation separation factors. This can be attributed to the more uniform synthesis conditions around the membrane support provided by the flow of the synthesis solution.

The effect of number of synthesis steps on separation factors, ideal selectivities and fluxes was investigated. For membranes synthesized in the flow system, consecutive synthesis yielded higher separation factors and ideal selectivities, but lower fluxes. The non-zeolite pores in the first layer were effectively patched by consecutive synthesis.

Synthesis in a flow system, which is a novel method for synthesis of zeolite membranes, yielded membranes with comparable separation factors and fluxes in pervaporation separations and comparable ideal selectivities in gas permeation with literature. Considering the high ideal selectivities and good pervaporation separation factors, it can be concluded that synthesis in the flow system is a promising method for synthesis of MFI type zeolite membranes.

## RECOMMENDATIONS

Pervaporation separation performance of membranes synthesized in a flow system was investigated. In addition to what has been done in this study, suggestions on further work to be done are as follows:

- Membrane synthesis conditions can be improved to have reproducible membrane synthesis. Precautions can be taken against temperature gradients.
- Pure component pervaporation fluxes of dimethyl benzene or triisopropyl benzene can be measured to have an idea about the dimensions of the defects in the membranes.
- Membrane synthesis can be performed on a stainless steel support. By this way the aluminum incorporation to the zeolite framework can be prevented and higher separation factors might be obtained.
- Synthesis can be performed on more complex support geometries such as monoliths.

## REFERENCES

1. D.W.Breck, "Zeolite molecular sieves: Structure, chemistry, and use", Wiley, New York, 1974.
2. T. C. Bowen, R. D. Noble, J. L. Falconer, *J. Membr. Sci.* 245 (2004) 1–33.
3. Y.Morigami, M.Kondo, J.Abe, H.Kita, K.Okamoto, *Sep.Purif.Technol.* 25 (2001) 251.
4. M. Noack, P. Kölsch, R. Schäfer, P. Toussaint, J. Caro, *Chem. Eng. Technol.* 25 (2002) 3.
5. M. Noack, P. Kölsch, J.Caro, M.Schneider, P. Toussaint, I. Sieber, *Micropor. Mesopor. Mater.* 35-36 (2000) 253.
6. S. H. Hyun, J. K. Song, B.J. Kwak, J. H. Kim, S. A. Hong, *J. Mater. Sci.* 34 (1999) 3095.
7. M. Nomura, T. Yamaguchi, S. Nakao, *J. Membr. Sci.* 144 (1998) 161-171.
8. J. Hedlund, B. J. Schoeman, J. Sterte, H. Chon, S. K. Ihm, Y. S. Uh, *Stud. Surf. Sci. Catal.* 105 (1997) 2203.
9. L. Gora, J.C. Jansen, Th. Maschmeyer, *Chem. Eur. J.* 14 (2000) 2539.
10. B. J. Schoeman, J. Sterte, J. E. Otterstedt, *J. Chem. Soc. Chem. Commun.* (1993) 994.
11. M. C. Lovallo, A. Gouzinis, M.Tsapatsis, *AIChE J.* 44 (1998) 1903.
12. S. Li, V. A. Tuan, J. L. Falconer, R. D. Noble, *Micropor. Mesopor. Mater.* 58 (2003) 137–154.
13. X.Chen, Z.Ping, Y.Long, *J.App.Poly.Sci.* 67 (1998) 629.
14. H.Matsuda, H.Yanagishita, D.Kitamoto, T.Nakae, K.Haraya, N.Koura, F.Mizukami, K.Haraya, T.Sano, *Membrane* 23 (1998) 259.
15. M.P. Pina, M. Arruebo, M. Felipe, F. Fleta, M.P. Bernal, J. Coronas, M. Menendez, J. Santamaria, *J. Membr.Sci.* 244 (2004) 141.

16. H. Richter, I. Voigt, G. Fischer, P. Puhlfurß, *Sep. Purif. Technol.* 32 (2003) 133.
17. P.Z. Çulfaz, A.Çulfaz, H.Kalıpçılar, *Micropor. Mesopor. Mater.*92 (2006) 134–144.
18. M.Mulder, ‘Basic Principles of Membrane Technology’, Kluwer Academic Publishers, Dordrecht, 1996
19. A. I. Skoulidas, D. S. Sholl, *AIChE J.* 51 (2005) 867- 877.
20. A. Giaya, R.W. Thompson, R. Denkewicz, *Micropor. Mesopor. Mater.* 40 (2000) 205.
21. F. Fajula, D. Plee, *Stud. Surf. Sci. Catal.* 85 (1994) 633.
22. T. Sano, H. Yanagishita, Y. Kiyozumi, F.Mizukami,K.Haraya, *J.Mem.Sci.* 95 (1994) 221.
23. M.A. Cambor, A. Corma, S. Iborra, S. Miquel, J. Primo, S. Valencia, *J. Catal.*, 172 (1997) 76.
24. J. Caro, M. Noack, P. Kölsch, R. Schäfer, *Micropor. Mesopor. Mater.* 38 (2000) 3.
25. F. Jareman, Doctoral Thesis submitted to Department of Chemical Engineering and Geosciences, Lulea University of Technology, 2004
26. E.E. McLeary, J.C. Jansen, F. Kapteijn, *Micropor. Mesopor. Mater.* 90 (2006) 198–220.
27. M. Pan, Y.S. Lin, *Micropor. Mesopor. Mater.* 43 (2001) 319.
28. H.Hart, L.E. Craine, D.J.Hart, *Organic Chemistry*, Houghton Mifflin Company, New York, 1999
29. J. Hedlund, J. Sterte, M. Anthonis, A.-J. Bons, B. Carstensen, N. Corcoran, D. Cox, H. Deckman, W.D. Gijnst, P.P. de Moor, F. Lai, J. McHenry, W. Mortier, J. Reinoso, J. Peeters, *Micropor. Mesopor. Mater.* 52 (2002) 179.
30. Z.P. Lai, G. Bonilla, I. Diaz, J.G. Nery, K. Sujaoti, M.A. Amat, E. Kokkoli, O. Terasaki, R.W. Thompson, M. Tsapatsis, D.G. Vlachos, *Science*, 300 (2002) 456

31. T.C. Bowen, H. Kalipcilar, J.L. Falconer, R.D. Noble, *J. Membr. Sci.* 215 (2003) 235.
32. X. Lin, H. Kita, K. Okamoto, *Chem. Comm.* 19 (2000)1889.
33. Y. Satoshi, S. Tsutsumi, *Micropor. Mesopor. Mater.* 37 (2000) 67.
34. Mitsui Engineering and Shipbuilding Co. Ltd., *Bulletin*, January 2004  
<http://www.mes.co.jp>, last accessed on 14<sup>th</sup> May 2007
35. M. Kondo, M. Komori, H. Kita, K. Okamoto, *J. Membr. Sci.* 133 (1997) 133.
36. S.M. Holmes, M. Schmitt, C. Markert, R.J. Plaisted, J.O. Forrest, P.N. Sharratt, A.A. Garforth, C.S. Cundy, J. Dwyer, *Chem. Eng. Res. Design* 78 (2000) 1084.
37. Okamoto, H. Kita, K. Horii, K. Tanaka, M. Kondo, *Ind. Eng. Chem. Res.*, 40 (2001) 163.
38. Y.Li, X.Zhang, J.Wang, *Sep.and Purif.Tech.* 25 (2001) 459-466
39. W. Jia, S. Murad, *Molecular Physics*, 104 (2006) 3033–3043
40. X. Lin, X. Chen, H. Kita, K.-I. Okamoto, *AIChE J.*, 49 (2003)
41. Q. Liu, R.D. Noble, J.L. Falconer, H.H. Funke, *J. Membr.Sci.*, 117 (1996) 163.
42. H. Matsuda, H. Yanagishita, H. Negishi, D. Kitamoto, T. Ikegami, K. Haraya, T. Nakane, Y. Idemoto, N. Koura, T. Sano, *J. Membr. Sci.* 210 (2002) 433.
43. T.C. Bowen, S. Li, R.D. Noble, J.L. Falconer, *J. Membr. Sci.*, 225 (2003)165.
44. T. Sano, M. Hasegawa, Y. Kawakami, H. Yanagishita, *J. Membr. Sci.*, 107 (1995) 193.
45. C.L. Flanders, V.A. Tuan, R.D. Noble, J.L. Falconer, *J. Membr. Sci.*, 176 (2000) 43.
46. W. Yuan, Y.S. Lin, W. Yang, *J. Am.Chem. Soc.*, 126 (2004) 4776.
47. K.Scott, *Ethanol Today*, February 2004



48. T.Sano, S.Ejiri, K.Yamada, Y.Kawakami, H.Yanagiishita, *J.Memb.Sci.*, 123 (1997) 225-233
49. V.A.Tuan, S.Li, J.L.Falconer, R.D.Noble, *J.Memb.Sci.*, 196 (2002) 111-123
50. X.Lin, H.Kita, K.Okamoto, *Ind.Eng.Chem.*, 40 (2001) 4069-4078
51. M.Nomura, T.Bin, S.Nakao, *Sep.Purif.Tech.*, 27 (2002) 59-66
52. J.M. van de Graaf, E. van der Bijl, A. Stol, F. Kapteijn, J.A. Moulijn, *Ind. Eng. Chem. Res.*, 37 (1998) 4071.
53. H. Takaba, A. Koyama, S. Nakao, *J. Phys. Chem. B*, 104 (2000) 6353.
54. T. Sano, T. Kasuno, K. Takeda, S. Arazaki, Y. Kawakami, *Stud. Surf. Sci. Catal.*, 105 (1997) 1771.
55. Y. Oumi, A. Miyajima, J. Miyamoto, T. Sano, *Stud. Surf. Sci. Catal.*, 142 (2002) 1595.
56. Z.A.E.P. Vroon, K.Keizer, M.J.Gilde, H.Verweij, A.J.Burggraaf, *J. Membr. Sci.*, 113 (1996) 293-300
57. Hedlund, J., Jareman, F., Bons, A., Anthonis, M., *J.Memb.Sci.*, 222 (2003) 163
58. Vroon, Z.A.E.P., Keizer, K., Burggraaf, A.J., Verweij, H., *J.Memb.Sci.*, 144 (1998) 65
59. Schoeman, B.J., E.Şenatalar, A., Hedlund, J., Sterte, J., *Zeolites*, 19 (1997) 21-28.
60. Funke, H.H., Kovalchick, M.G., Falconer, J.L., Noble, R.D., *Ind. Eng. Chem. Res.*, 35 (1996) 1575-1582.
61. Oonkhanond, B., Mullins, M.E., *J.Memb.Sci.*, 194 (2001) 3-13.
62. F.Jareman, J.Hedlund, D.Creaser, J.Sterte, *J. Membr. Sci.*, 236 (2004) 81-89
63. J.M.van de Graaf, F.Kapteijn, J.A.Moulijn, *Microp.Mesop.Mater.* 35-36 (2000) 267-281
64. J. Coronas, J.L. Falconer, R.D. Noble, *AIChE J.* 43 (7) (1997) 1797.

65. Kang B.S., Gavalas, G.R., *Ind. Eng. Chem. Res.* 41 (2002) 3145-3150.
66. V.A. Tuan, J.L. Falconer, R.D. Noble, *Ind. Eng. Chem. Res.* 38 (1999) 3635.
67. J.Hedlund, M.Noack, P.Kölsch, D.Creaser, J.Caro, J.Sterte, *J. Membr. Sci.* 159 (1999) 263-273
68. K. Weh, M. Noack, I. Sieber, J. Caro, *Microp.Mesop. Mater.* 54 (2002) 27–36
69. M.P. Bernal, J.Coronas, M.Menendez, J.Santamaria, *AIChE J.* 50 (2004) 1
70. A.J.Burgraaf, Z.A.E.P.Vroon, K.Keizer, H.Verweij, *J. Membr. Sci.* 144 (1998) 77-86
71. N.Nishiyama, L.Gora, V. Teplyakov, F.Kapteijn, J.A.Moulijn, *Sep.and Purif. Tech.* 22-23 (2001) 295-307
72. J.M. van deGraaf, F.Kapteijn, J.A.Moulijn, *J. Membr. Sci.* 144 (1998) 87.
73. A.J. Burgraaf, *J. Membr. Sci.* 155 (1999) 45.
74. W.Zhu, P. Hrabanek, L. Gora, F. Kapteijn, J.A. Moulijn, *Ind.Eng.Chem.Res.* 45 (2006) 767-776.
75. J.Dong, Y.S.Lin, *AIChE J.* 46 (2000) 10
76. C.Algieri, P.Bernardo, G.Golemme, G.Barbieri, E.Drioli, *J. Membr. Sci.* 222 (2003) 181-190
77. W.J.W.Bakker, L.J.P. Van den Broeke, F. Kapteijn, J.A.Moulijn, *AIChE J.* 43 (1997) 2203
78. C.J.Gump, X.Lin, J.L. Falconer, R.D.Noble, *J. Membr. Sci.* 173 (2000) 35-52
79. F.Jareman, J.Hedlund, J.Sterte, *Sep.and Purif. Tech.* 32 (2003) 159-163
80. G.Xomeritakis, A.Gouzinis, S.Nair, T.Okubo, M.He, R. M. Overney, M.Tsapatsis, *Chem.Eng.Sci.* 54 (1999) 3521-3531
81. P.Z.Çulfaz, Thesis submitted to graduate school of Natural and Applied Sciences of Middle East Technical University, June 2005
82. E.Dinçer, Thesis submitted to graduate school of Natural and Applied Sciences of Middle East Technical University, July 2005

## APPENDIX A

### CALIBRATION PLOTS FOR THE PERVAPORATION MEASUREMENTS

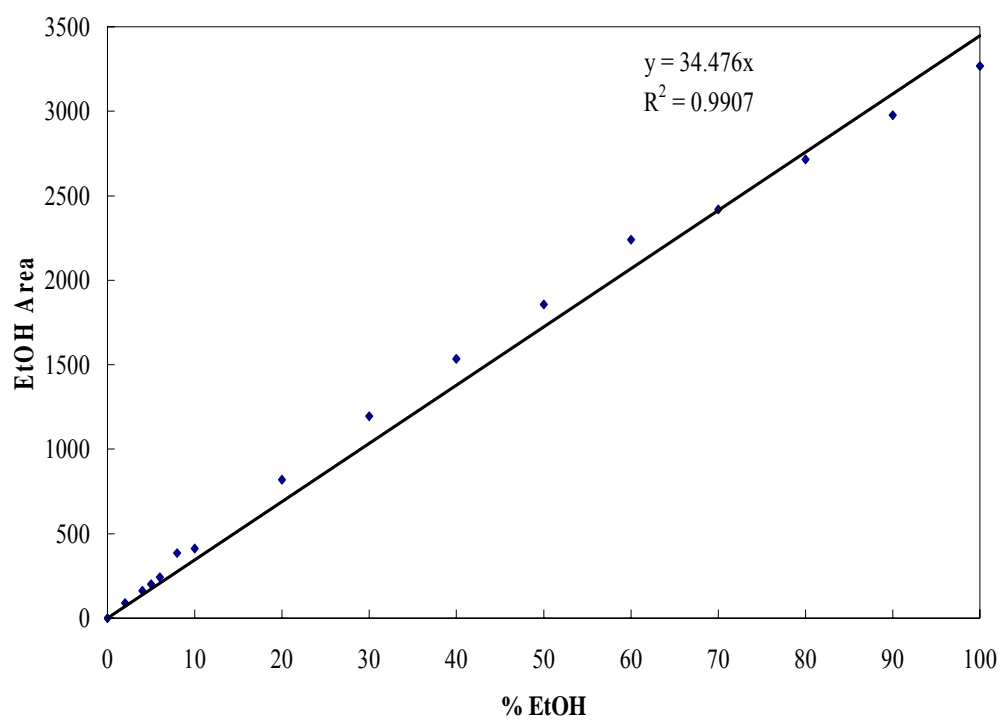


Figure A.1. Variation of ethanol peak area with ethanol concentration in ethanol/water mixture (wt%)

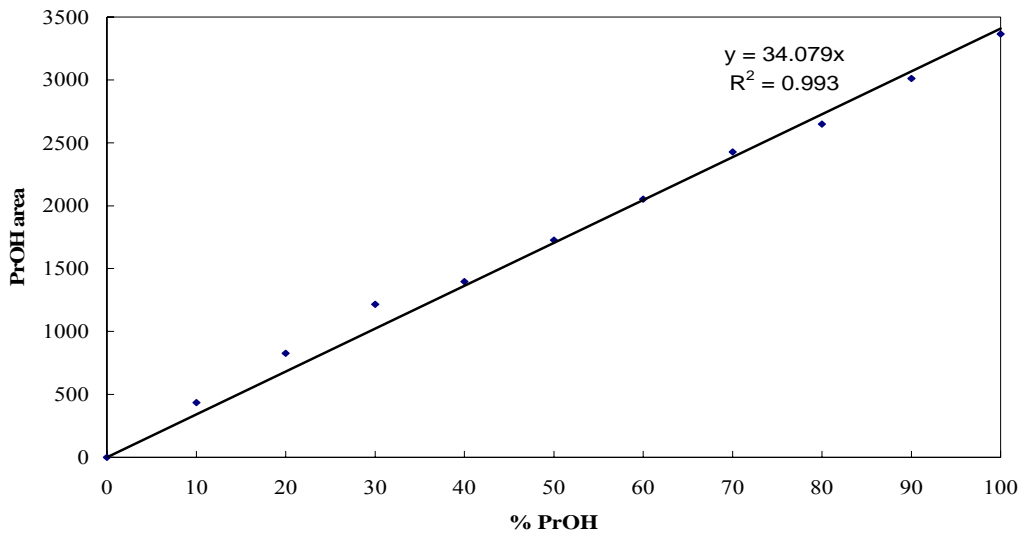


Figure A.2. Variation of 2-Propanol peak area with 2-propanol concentration in propanol/water mixture (wt%)

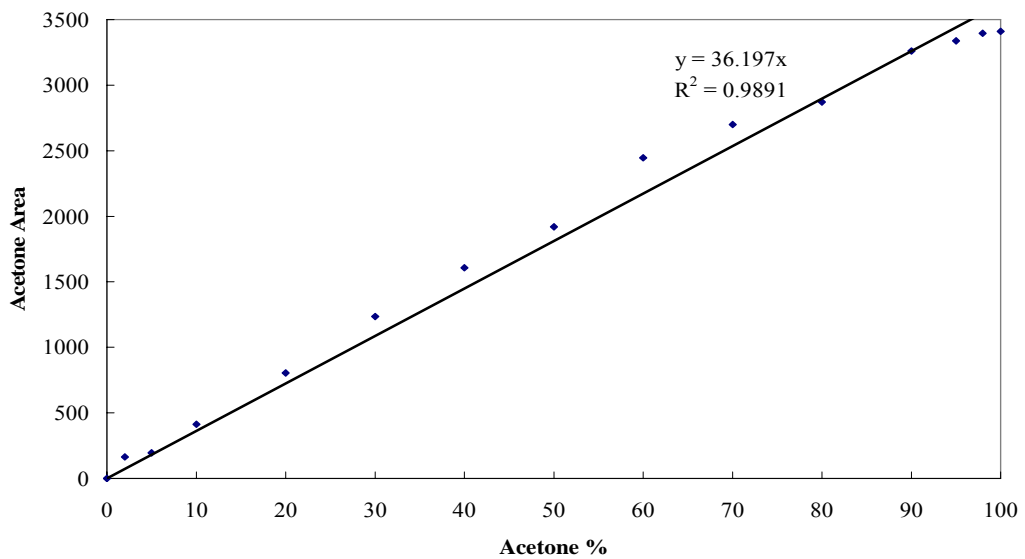


Figure A.3. Variation of acetone peak area with acetone concentration in acetone/water mixture (wt%)

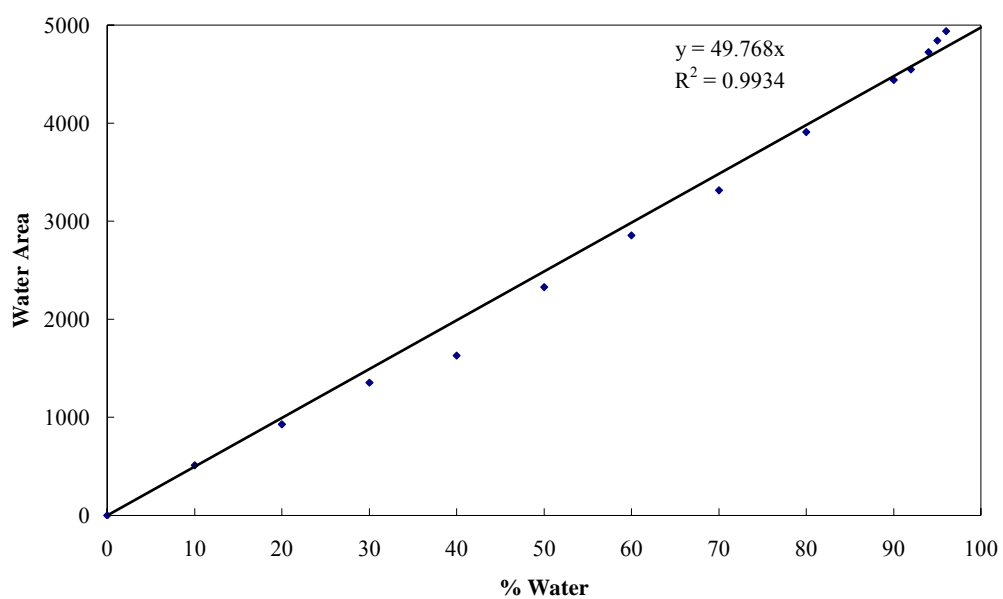


Figure A.4. Variation of water peak area with water concentration in organic/water mixture (wt%)

## APPENDIX B

### RAW DATA FOR GAS PERMEATION EXPERIMENTS

Table B.1. Gas permeabilities ( $\text{mol/m}^2 \cdot \text{Pa} \cdot \text{s} \times 10^7$ ) at 25 °C

Gas/Membrane	F1	F2	F3	B2	B1	F4
H <sub>2</sub>	6.24	1.66	3.54		15.9	4.07
CO <sub>2</sub>	10.15	2.41	6.65	4.06	34.6	8.00
N <sub>2</sub>	4.55	1.26	2.32	1.67	23.8	2.68
CH <sub>4</sub>	11.40	5.65	5.89	3.63	42.3	11.2
n-C <sub>4</sub>	2.06	0,004	0.27	0.007	2.32	0.02
i-C <sub>4</sub>	0.75	0,004	0.002	0.007	0.38	0.003

Table B.2. Gas permeabilities ( $\text{mol/m}^2 \cdot \text{Pa} \cdot \text{s} \times 10^7$ ) at 200 °C

Gas/Membrane	F1	F2	F3	B2	B1	F4
H <sub>2</sub>	5.97	1.53	3.03	1.05	19.8	3.44
CO <sub>2</sub>	3.92	1.36	2.92	1.91	15.6	3.08
N <sub>2</sub>	2.61	0.82	1.47	1.30	10.1	1.67
CH <sub>4</sub>	4.66	1.66	2.53	2.45	18.6	3.43
n-C <sub>4</sub>	4.02	0.77	2.12	1.36	14.8	2.78
i-C <sub>4</sub>	0.43	0.006	0.01	0.11	0.30	0.02

## APPENDIX C

### RAW DATA FOR PERVAPORATION EXPERIMENTS

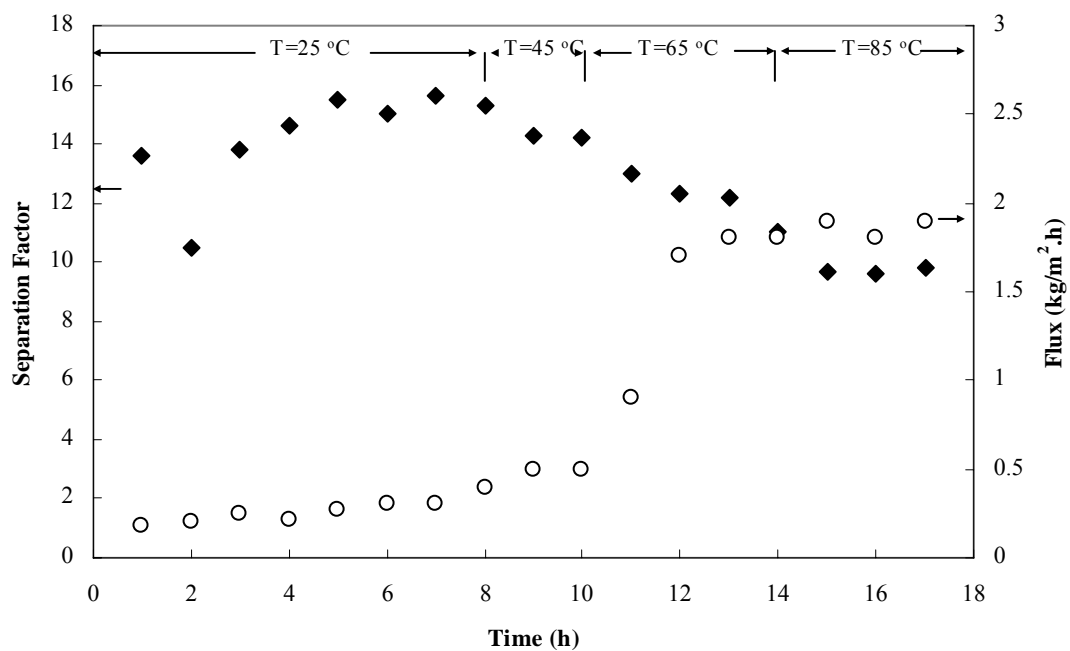


Figure C.1. Variation of separation factor and flux for membrane F1 for 5 wt% ethanol/water solution

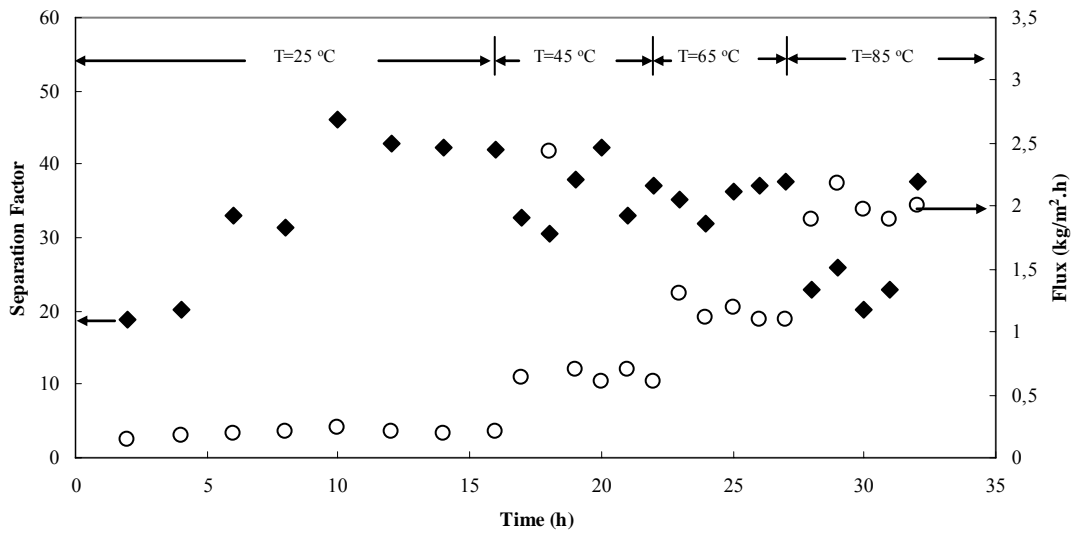


Figure C.2. Variation of separation factor and flux for membrane F2 for 5 wt% ethanol/water solution

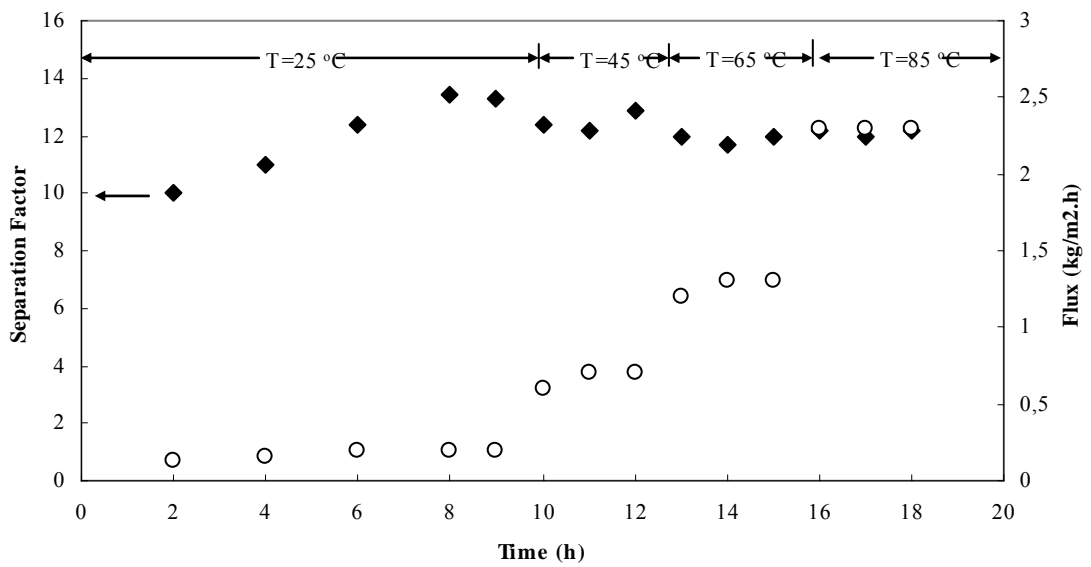


Figure C.3. Variation of separation factor and flux for membrane F3 for 5 wt% ethanol/water solution



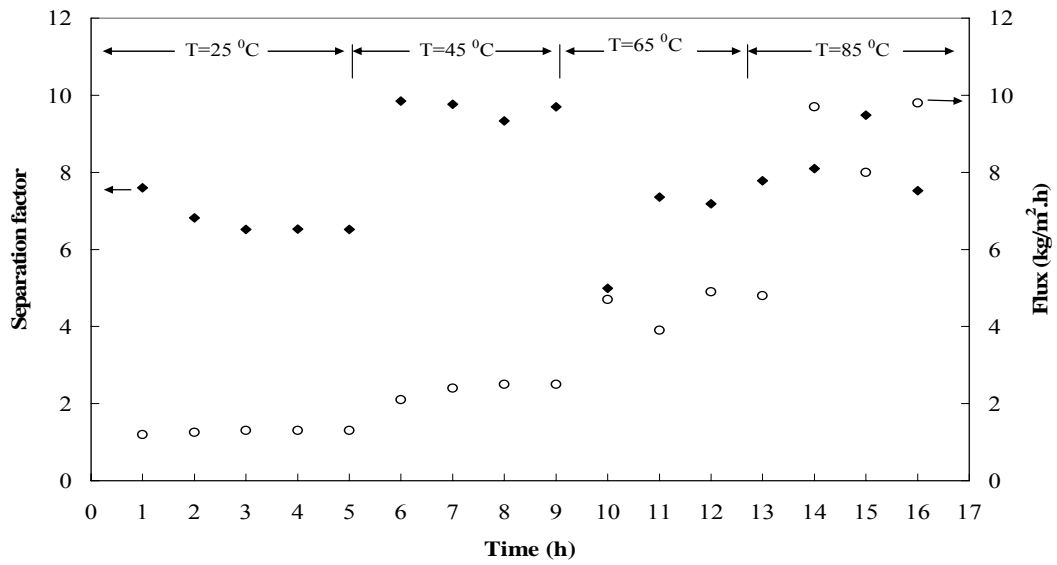


Figure C.4. Variation of separation factor and flux for membrane B1 for 5 wt% ethanol/water solution

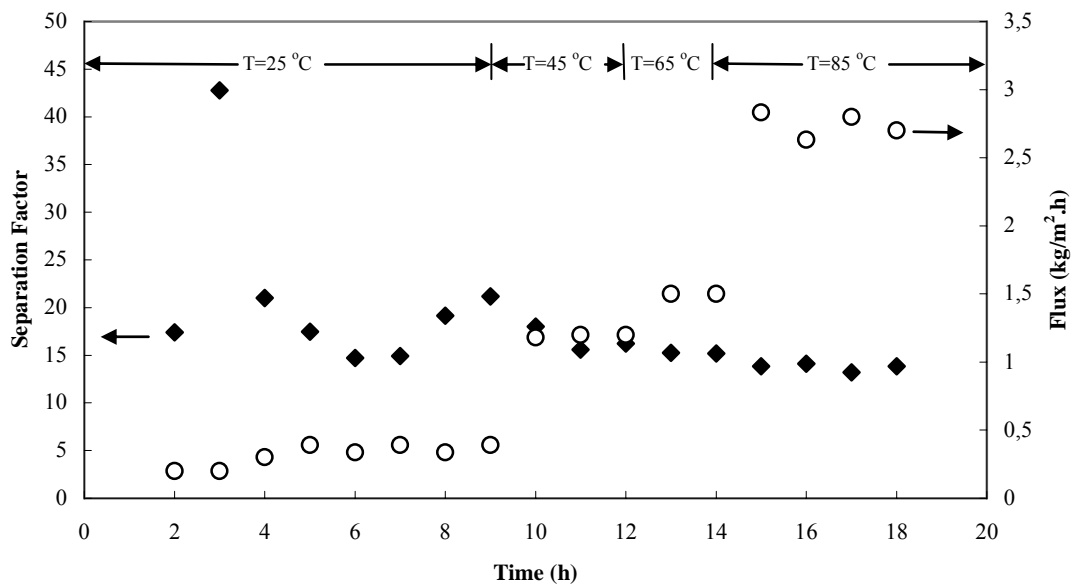


Figure C.5. Variation of separation factor and flux for membrane B2 for 5 wt% ethanol/water solution

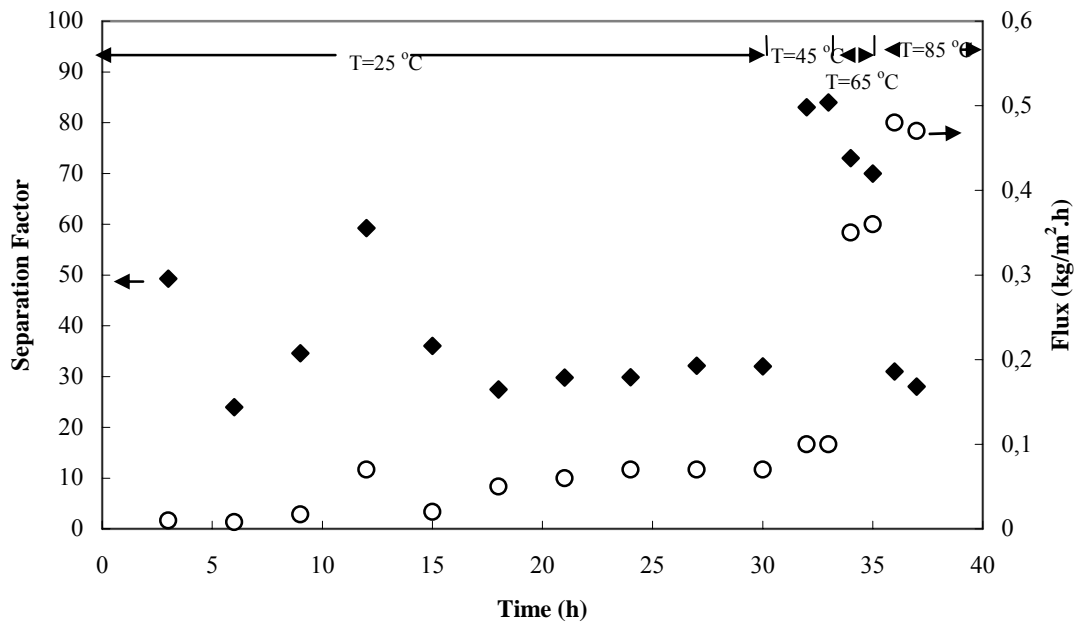


Figure C.6. Variation of separation factor and flux for membrane F2 for 5 wt% 2-propanol/water solution

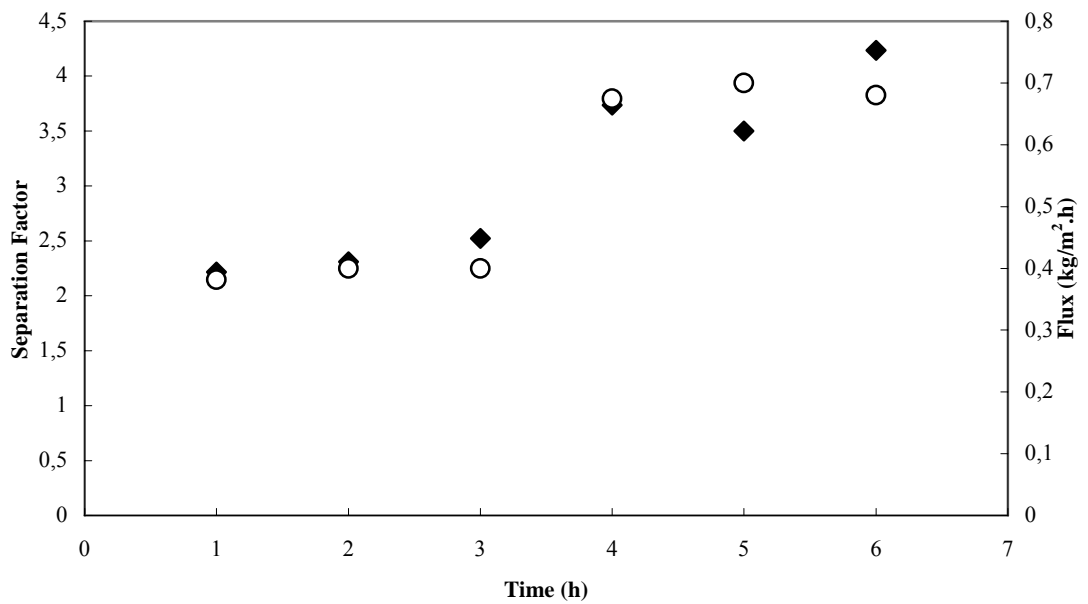


Figure C.7. Variation of separation factor and flux for membrane F1 for 5 wt% 2-propanol/water solution at room temperature

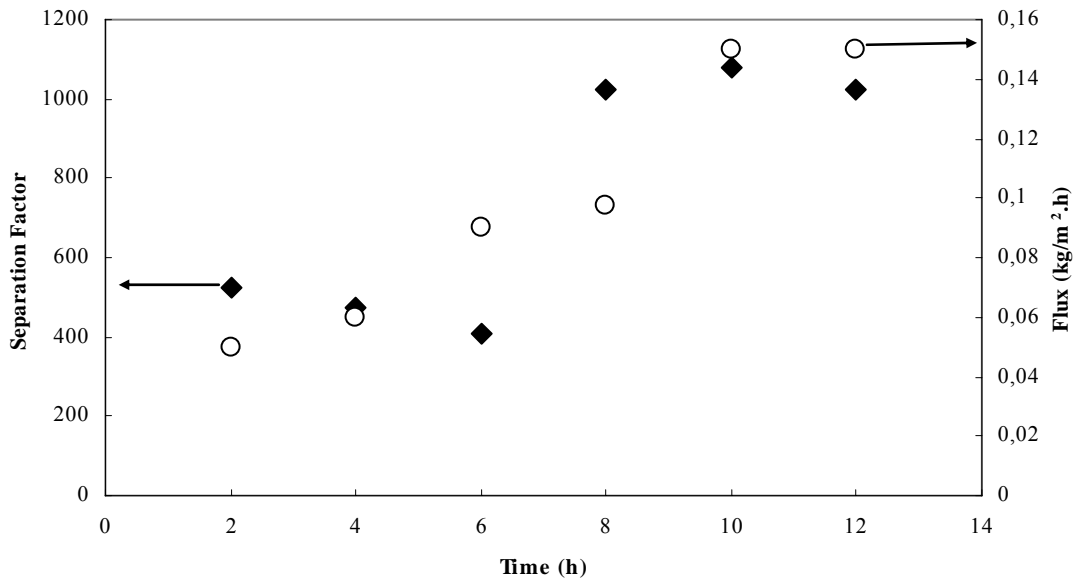


Figure C.8. Variation of separation factor and flux for membrane F2 for 5 wt% 2-acetone/water solution at room temperature

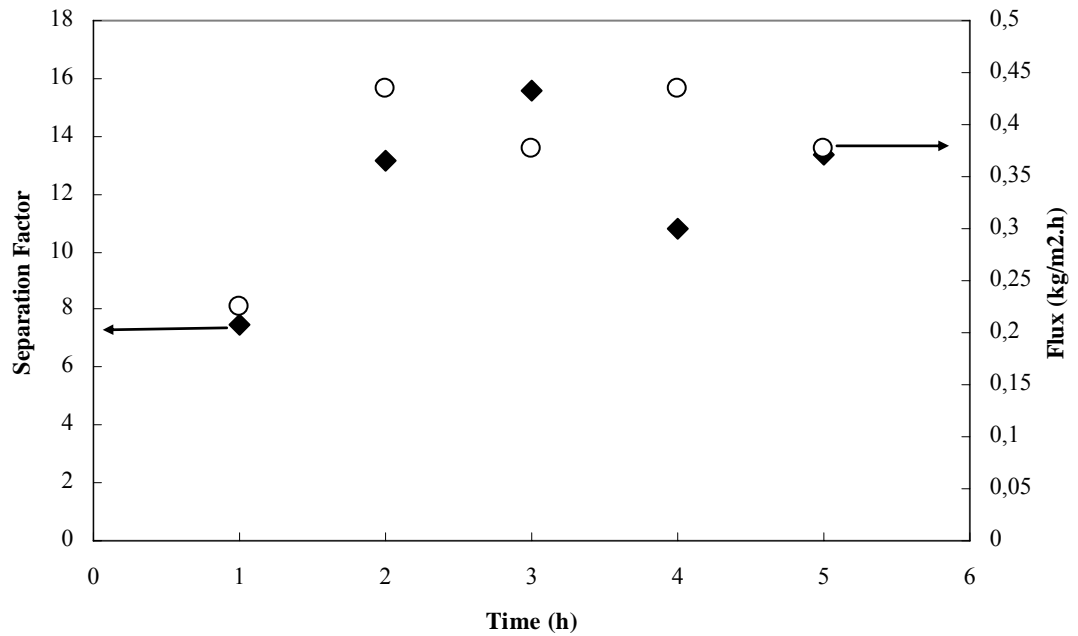


Figure C.9. Variation of separation factor and flux for membrane F1 for 5 wt% 2-acetone/water solution at room temperature

## **APPENDIX D**

### **PHOTOGRAPHS OF THE PERVAPORATION SET-UP**

Figure D.1. Photographs of the pervaporation set-up

## APPENDIX E

### REFERENCES FOR FIGURE 4.12

1. V.A.Tuan, S.Li, J.L.Falconer, R.D.Noble, J.Memb.Sci., 196 (2002) 111-123
2. Q. Liu, R.D. Noble, J.L. Falconer, H.H. Funke, J. Membr.Sci., 117 (1996) 163.
3. T.Sano, S.Ejiri, K.Yamada, Y.Kawakami, H.Yanagishita, J.Memb.Sci., 123 (1997) 225-233
4. T.C. Bowen, H. Kalipcilar, J.L. Falconer, R.D. Noble, J. Membr. Sci. 215 (2003) 235.
5. H. Matsuda, H. Yanagishita, H. Negishi, D. Kitamoto, T. Ikegami, K. Haraya, T. Nakane, Y. Idemoto, N. Koura, T. Sano, J. Membr. Sci. 210 (2002) 433.
6. H.Matsuda, H.Yanagishita, D.Kitamoto,K. Haraya, T.Nakane,T.Takada, Y.Idemoto, N.Koura, T.Sano, Sep. Sci. Tech. 36 (15) (2001) 3305-3310.
7. X.Lin, H.Kita, K.Okamoto, Ind.Eng.Chem. 40 (2001) 4069-4078.
8. T. Sano, M. Hasegawa, Y. Kawakami, H. Yanagishita, J. Membr. Sci., 107 (1995) 193.

9. X. Lin, H. Kita, K. Okamoto, Chem. Comm. 19 (2000)1889.
10. X. Lin, X. Chen, H. Kita, K. Okamoto, AIChE J. (2003) 49.
11. M. Nomura, T. Yamaguchi, S. Nakao, J. Memb. Sci. 144 (1998) 161.